



Early View

Original article

β 2 integrin LFA1 mediates airway damage following neutrophil trans-epithelial migration during RSV infection

Jenny Amanda Herbert, Yu Deng, Pia Hardelid, Elisabeth Robinson, Luo Ren, Dale Moulding, Rosalind Louise Smyth, Claire Mary Smith

Please cite this article as: Herbert JA, Deng Y, Hardelid P, *et al.* β 2 integrin LFA1 mediates airway damage following neutrophil trans-epithelial migration during RSV infection. *Eur Respir J* 2020; in press (<https://doi.org/10.1183/13993003.02216-2019>).

This manuscript has recently been accepted for publication in the *European Respiratory Journal*. It is published here in its accepted form prior to copyediting and typesetting by our production team. After these production processes are complete and the authors have approved the resulting proofs, the article will move to the latest issue of the ERJ online.

Title: β 2 integrin LFA1 mediates airway damage following neutrophil trans-epithelial migration during RSV infection.

Short summary: Neutrophils reduce RSV load but their adherence to airway epithelial cells via β 2 integrin LFA1 inflicts collateral airway damage.

Authors: Jenny Amanda Herbert¹, Yu Deng^{1,2}, Pia Hardelid¹, Elisabeth Robinson¹, Luo Ren^{1,2}, Dale Moulding¹, Rosalind Louise Smyth^{1†}, Claire Mary Smith^{1†*}.

Affiliations:

¹ UCL Great Ormond Street Institute of Child Health, London, UK.

² Department of Respiratory Medical Centre, Chongqing Key Laboratory of Child Infection and Immunity, Children's Hospital of Chongqing Medical University, China International Science and Technology Cooperation base of Child development and Critical Disorders, Ministry of Education Key Laboratory of Child Development and Disorders, Chongqing, 400014, China.

* corresponding author: Dr Claire M Smith, UCL Great Ormond Street Institute of Child Health, 30 Guilford St, London WC1N 1EH, c.m.smith@ucl.ac.uk

† joint senior author.

Manuscript word count 3998

Abstract

RSV bronchiolitis is the most common cause of infant hospital admissions, but there is limited understanding of the mechanisms of disease and no specific anti-viral treatment. Using a novel *in vitro* primary trans-epithelial neutrophil migration model and innovative imaging methods, we show that RSV infection of nasal airway epithelium increased neutrophil trans-epithelial migration and adhesion to infected epithelial cells, which is associated with epithelial cell damage, reduced ciliary beat frequency, but also a reduction in infectious viral load.

Following migration, RSV infection results in greater neutrophil activation, degranulation and release of neutrophil elastase into the airway surface media compared to neutrophils that migrated across mock-infected nasal epithelial cells. Blocking of the interaction between the ligand on neutrophils (the β 2 integrin LFA-1) for intracellular adhesion molecule-1 (ICAM-1) on epithelial cells reduced neutrophil adherence to RSV infected cells and epithelial cell damage to pre-infection levels, but did not reduce the numbers of neutrophils which migrated or prevent the reduction in infectious viral load.

These findings have provided important insights into the contribution of neutrophils to airway damage and viral clearance, which are relevant to pathophysiology of RSV bronchiolitis. This model is a convenient, quantitative pre-clinical model that will further elucidate mechanisms that drive disease severity and has utility in anti-viral drug discovery.

Abstract word count 207 (max 250)

Introduction

Respiratory syncytial virus (RSV) is the leading cause of bronchiolitis and the most prevalent viral cause of hospitalisation in children under 1 year of age [1]. There is currently no vaccine to prevent RSV infection and no specific anti-viral treatment. Recent advances in structural biology have revived RSV vaccine and anti-viral development, with several vaccines [2] and anti-viral candidates [3–5] coming through the therapeutic pipeline. Expanding our understanding of the mechanisms that underlie the pathophysiology of RSV bronchiolitis is important to support the development of RSV-specific therapies. Studies using *in vitro* human ciliated airway epithelial cell models of RSV infection have led to important insights into host responses to respiratory viruses [6–9]. However, unlike lung tissue from infants with RSV [10, 11], these *in vitro* models reveal few signs of cytopathology during RSV infection, which raises doubt about their utility when studying the pathophysiology of RSV bronchiolitis in infants.

Neutrophils are the predominant immune cell recruited to the lungs of infants with RSV bronchiolitis [12, 13]. Their role in host defence is not fully understood. We hypothesised that migration of neutrophils across RSV infected nasal airway epithelial cells (nAEC) contributes to cellular damage and reveal important host response mechanisms. We previously developed a neutrophil migration model [14, 15] using a human alveolar type II cell line (A549), which is commonly used to study RSV infection *in vitro* [15–17]. However, ciliated AECs are the main target for RSV infection and immortalised cell lines often lack appropriate cell polarisation and many other important properties found in the airway, such as mucus. Therefore, in order to interrogate neutrophil trans-epithelial migration further, we have developed a more physiologically relevant *in vitro* model using primary human nasal epithelial cells grown at the air-liquid interface (ALI) (Figure 1). Here we seed primary AECs

on the underside of porous membrane inserts, rather than the topside as in conventional ALI culture. This is because, although there is some suggestion that neutrophil migration can occur against gravity, our preliminary studies indicated that the numbers of neutrophils recovered is very low (about 2500 cells). Our gravity-fed system, has demonstrated to be an ideal system to study neutrophil function following trans-epithelial migration. Here we observed neutrophil chemotaxis across primary differentiated nAECs and, for the first time, we measured neutrophil adherence and the associated epithelial damage including ciliary beat frequency, a sensitive assessment of cellular toxicity.

Materials and Methods

Participants

Peripheral blood and airway epithelial cells were obtained from healthy adult donors at UCL GOS Institute of Child Health. Written informed consent was obtained from all donors prior to their enrolment in the study. Study approval was obtained from the UCL Research Ethics Committee (4735/002). All methods were performed in accordance with the relevant guidelines and regulations.

Virus purification and quantification

Recombinant (rg) RSV A2 strain that possesses a GFP tagged large (L) polymerase that expresses GFP in epithelial cells that are replicating virus, was kindly provided by Fix et al [18]. Viral stock preparation and quantification of viral titre from serially diluted nAEC supernatants was performed using HEp-2 cells (ATCC CCL-23) as described previously [14, 15]. Quantitative RT-PCR was performed using TaqMan Universal Master Mix II, with UNG (Applied Biosystems). A total volume of 20µl was used with 1µl of cDNA per reaction. Primers, probes and reaction conditions were used as previously described [14, 19]. A plasmid containing the N protein sequence [20] was used to quantify the N protein copy number in nAEC supernatant and from within cells. RSV load was extrapolated from a standard curve of known N protein copies.

Neutrophil trans-epithelial migration assay

Primary airway epithelial cells were obtained from nasal brushings as described previously [21] or purchased from Epithelix Sàrl (Switzerland). A diagram of our methodology is shown in **Figure 1** and a detailed protocol for nAECs culture can be found in Supplementary Methods. We found no difference in the cultures grown from a brushing or from commercial

supplier (see Supplementary **Figure S1**). Briefly, progenitor basal cells were propagated in co-culture with 3T3-JF mouse fibroblast feeder layers as described previously [22]. Primary nAECs are seeded into feeder layers at a density of 5×10^5 / flask in F-media (DMEM and Hams F12 media at a 3:1 ratio supplemented with $1 \times$ Penicillin streptomycin, 7.5% fetal bovine serum (Gibco), 5 mM Y-27632 (Abcam), 25 ng/ml hydrocortisone/ 0.125 ng/ml epidermal growth factor (Sigma), 5 mg/ml insulin (Sigma), 0.1 nM cholera toxin (Sigma) and amphotericin B (2.50 μ g/ml)) and cultured until confluent. Primary nAECs and 3T3-J2 fibroblasts were then separated by differential trypsin dissociation as previously described [22]. Basal cells were collected in fresh F-media and centrifuged at 200xg for 3 minutes.

Collagen coated 3 μ m pore membrane inserts (ThinCert, Griener, with culture surface of 33.6 mm²) were inverted and 300,000/cm² nAECs in 70 μ l of F-media were seeded onto the bottom of the insert and incubated at 37°C 5% CO₂ for 4-6 hours. After incubation membrane inserts were inverted into a 24 well plate and 500 μ l of fresh F-media added underneath and 100 μ l of F-media supplemented with 30 μ g/ml Collagen I and 5% (v/v) Matrigel added to the top of the membrane inserts. Cells were incubated for 24-48 hours at 37°C 5 % CO₂. After this period cells were put at ALI. Media was aspirated from both sides of the membrane insert and cells fed basolaterally with 100 μ l of ALI media (1:1 DMEM: airway epithelial cell growth media (PromoCell), with all supplements added, further supplemented with 2.5 μ g/ml Amphotericin B, 1x penicillin/ streptomycin and 1 μ m retinoic acid (Sigma)). Media was replaced every 1-2 days, and cells incubated at 37°C 5% CO₂ in a high humidity incubator for 4 weeks/ 28 days to allow cellular differentiation. Once differentiated, cells were infected with RSV as before [19].

Neutrophils were purified from 10ml of peripheral venous blood using a negative immunoselection neutrophil isolation kit (STEMCELL Technologies), as per the manufacturer instructions. The mean number of neutrophils isolated from was 1.5×10^7 cells with a purity of 99.8-99.9% as confirmed by flow cytometry (See **Figure S1D**). Neutrophils were stained with CellTrace Calcein Red-Orange cell stain (ThermoFisher) as described previously [14].

For neutrophil trans-epithelial migration 400 μ l of apical surface media was placed underneath the membrane insert for each experimental group; mock infected, RSV infected, mock infected exposed to apical surface media collected from RSV infected cells or N-Formylmethionine-leucyl-phenylalanine (fMLP). To investigate the interaction of the integrin leukocyte function-associated antigen-1F (LFA1) with the cell adhesion molecule ICAM-1, we supplemented the apical surface media collected from RSV infected cells with 1 μ M (2E)-1-(4-Acetyl-1-piperazinyl)-3-[4-[[2-(1-methylethyl)phenyl]thio]-3-nitrophenyl]-2-propen-1-one (A286982, TOCRIS BioTechne), a potent antagonist (inhibitor) of the LFA-1 CD11a I domain [23]. A IC_{50} concentration of 35-44nM was used, based on that used in other studies [24, 25]. Neutrophils (5×10^5) were added to the basolateral side of membrane inserts and left to migrate for 1 or 4 hours. After migration, neutrophils were collected from the apical side of the epithelial cells for quantification (see below). Apical surface medias (containing epithelial secreted factors including cytokines) were collected and membrane inserts were fixed and stained for ICAM-1, acetylated tubulin (cilia) or adherent neutrophils (see below).

Definitions (Figure 1):

Basolateral– the neutrophils that remain in the basolateral side of the epithelium (top chamber) and do not trans-migrate across the epithelium. **Migrated** - the neutrophils that

trans-migrate across the epithelium and detach into apical surface media (bottom chamber).

Adherent neutrophils - the neutrophils that trans-migrate across the epithelium and remain adhered to the airway epithelial cells

ICAM1 expression analysis

ICAM1 expression levels on ciliated nAEC were quantified after RSV infection for 24 and 72h. Detailed methods on the staining procedure is provided in an online data supplement. Z-stacks were acquired on a confocal microscope (Zeiss LSM710) using a x40 objective with 5µm distance between each image and up to 50µm range.

Quantification of migrated and adherent neutrophils

The number of migrated neutrophils was quantified as described previously [14]. Flow cytometric analysis of CD11b expression on migrated and basolateral neutrophils was performed as described previously [14]. Images of adherent neutrophils were acquired on a confocal microscope (Zeiss LSM710) under a x40 objective. Neutrophils were counted using the ImageJ counting tool.

Quantification of epithelial damage

Cell damage was quantified by TEER, red dextran permeability, LDH release and by counting the number of epithelial remaining on membrane inserts as described previously [14], and in **Figure S2**. To determine ciliary beat frequency (CBF), plates were placed in an incubation chamber (37°C, 5% CO₂) attached to an inverted microscope system as described previously [9]. Videos were recorded using a ×20 objective and CMOS digital video camera (Hamamatsu) at a rate of 198 frames per second (an example video of a ciliated area shown

in **Video1**). For each condition, twelve areas per membrane insert were videoed. CBF (Hz) was calculated by fast Fourier transformation using ciliaFA software [26].

Statistical analysis

Differences between the same donor cells exposed to different test conditions were analysed by paired t-test. A paired two way ANOVA with Bonferroni correction was used when multiple comparisons were performed (GraphPad Prism v4.0). Validation of the tests used and data modelling was performed using StataSE 15 (see Supplementary statistics file).

Results

Our model (Figure 1) generated similar findings at both 24h and 72h post RSV infection and in the figures we show both time points, but in interests of readability and clarity, in the text below, we will refer only to the data collected 72h post-infection. For data on RSV infection of primary ciliated nAECs without neutrophil migration, see supplementary **Figure S2**.

RSV infection increases the number of neutrophils that migrate across ciliated nAECs and dissociate into the apical surface media

Using our differentiated primary airway nasal epithelial cell model (Figure 1) we examined the numbers of neutrophils that migrated across and dissociated from the epithelium by measuring the number of fluorescently labelled neutrophils in the apical surface media. We found that after 1h >2 fold more neutrophils migrated across ciliated epithelium infected with RSV for 72h with a mean [\pm SEM] of neutrophils $5.7 \times 10^4 [\pm 1.2 \times 10^4]$ migrated neutrophils/well compared to the mock-infected epithelium ($2.3 \times 10^4 [\pm 5.2 \times 10^3]$) (P=0.034) (**Figure 2B**) (24h data shown in **Figure 2A**). This is equivalent to 11.4% of the total neutrophils added for RSV infected epithelial cells and 4.6% for mock infected epithelial cells. After 4h of neutrophil migration, we found that 34% of neutrophils had migrated across epithelial cells infected with RSV for 72h ($1.7 \times 10^5 [\pm 1.3 \times 10^4]$), which was, again, >2 fold the number of neutrophils that migrated across mock-infected epithelium (15.8%) ($7.9 \times 10^4 [\pm 9 \times 10^3]$) (P=0.0009) (**Figure 2B**).

To investigate whether secreted factors from RSV infected epithelial cells were contributing to this increased migration of neutrophils, we measured the number of neutrophils that migrated across mock-infected epithelium incubated with apical surface media collected from RSV infected epithelial cells. We found no difference in the number of migrated neutrophils

1h after neutrophil migration across mock-infected epithelium compared to mock infected epithelial cells exposed to apical surface media from cells infected with RSV 72h post infection (**Figure 2B**). However, 4h after migration across mock infected epithelial cells exposed to apical surface media from cells infected with RSV for 72h ($1.4 \times 10^5 [\pm 1.3 \times 10^4]$) cells had migrated, which was 1.7 fold greater than across mock infected cells exposed to media alone ($7.9 \times 10^4 [\pm 9 \times 10^3]$) ($P=0.0008$).

RSV increases the number of neutrophils that remain adherent to the infected ciliated epithelium

We found that after 1h neutrophil migration the number (mean \pm SEM) of neutrophils adherent to 72h RSV infected epithelial cells ($2.6 \times 10^3 \pm 2.7 \times 10^2$ neutrophils/cm²) was >3 fold greater than the mock infected epithelium ($8.6 \times 10^2 \pm 1 \times 10^2$ neutrophils/cm²) ($P<0.0001$) (**Figure 2D**), with more adherent neutrophils at 72h after RSV infection, compared with that after 24h of RSV infection (**Figure 2C**) ($P<0.05$). Interestingly, we found that the number of adherent neutrophils was less 4h after neutrophil migration ($3.6 \times 10^2 \pm 7.4 \times 10^1$ neutrophils/cm²) (**Figure 2D**) compared to 1h ($2.6 \times 10^3 \pm 2.7 \times 10^2$ neutrophils/cm²) ($P<0.0001$), with similar differences 24h after RSV infection. This was specific to RSV infected epithelium, as mock-infected epithelium where the number of adherent neutrophils after 4h neutrophil migration ($8.8 \times 10^2 \pm 1 \times 10^2$ neutrophils/cm²) was at similar levels to that found a 1h ($9.2 \times 10^2 \pm 1 \times 10^2$ neutrophils/cm²). To investigate whether secreted factors from RSV infected epithelial cells were contributing to this increased neutrophil adherence, we measured the number of neutrophils that adhered to mock-infected epithelium incubated with apical surface media collected from RSV infected epithelial cells. We found that the addition of apical surface media, collected from RSV infected cells, to mock-infected epithelium did not increase

neutrophil adhesion and after 1h we detected 2-3 times fewer adherent neutrophils compared to the RSV infected epithelium ($P < 0.0001$) (**Figure 2C&D**).

Neutrophil trans-epithelial migration during RSV infection causes epithelial cell damage and reduces ciliary beat frequency

We did not detect any signs of epithelial damage following neutrophil trans-epithelial migration at 24h post RSV infection. This is shown in supplementary **Figure S3**. We also did not detect any increase in makers of epithelial damage after 1h of neutrophil migration across epithelium infected with RSV for 72h (**Figure 3B**). However, 4h after neutrophil trans-epithelial migration across epithelium infected with RSV for 72h, we detected larger gaps ($70.8 \pm 4.6\%$ area) in the RSV infected epithelial layer compared to the mock-infected ($61.6 \pm 6.0\%$ area) ($P < 0.0001$) (representative images shown in **Figure 3A**, quantitative data shown in **Figure 3B**). These gaps were associated with epithelial rounding, as observed using time-lapse microscopy (see supplementary **Video2**), a loss of epithelial cells (**Figure 3C**), an increase in LDH release (**Figure 3D**) which was greater in RSV-infected cultures compared to the mock infected ($P < 0.0001$). Interestingly, this epithelial cell loss did not correspond with an increase in red dextran flux (**Figure S4**) or decrease in TEER (**Figure 3E**). We also did not find any differences in TEER compared with the mock-infected cells exposed to either RSV infected apical surface media or fMLP (**Figure 3E**). To determine whether physical impediments, that could alter the red dextran and electrical current outputs, were compensating for the loss in epithelial cells, we microscopically observed the sub-epithelial layer (top of the membrane insert) overtime and found that after 4h, the basolateral neutrophils had accumulated as a sediment (**Figure S5**).

Using high speed video microscopy we investigated whether neutrophil migration alters ciliary activity, which is a sensitive indicator of cell toxicity. We found that 30 minutes after the addition of neutrophils, the mean (SD) ciliary beat frequency (CBF) of thirty six $2856\mu\text{m}^2$ ciliated areas of interest we imaged from cultures infected with RSV for 72h was 12.84 (0.79) Hz compared 15.06 (0.95) Hz to in RSV infected cultures without neutrophils (**Figure 4B**) ($P<0.05$). Although this was not statistically different, an absolute difference in CBF of 2Hz has been shown to be clinically significant in reducing mucociliary clearance [27]. Eight hours after the addition of neutrophils, the average CBF of the mock and RSV infected cultures appeared to recover to pre-neutrophil levels (**Figure 4B**). However, when examined closely, comparing an individual region of interest over time, it was clear that neutrophil migration led to far fewer areas (1.4% ROI compared to 40.3% in RSV infected cultures without neutrophils) demonstrating active beating cilia (defined as $>3\text{Hz}$) (**Figure 4C**).

Epithelial damage correlates with neutrophil degranulation and higher apical concentrations of neutrophil elastase

Neutrophils release several toxic products, including myeloperoxidase (MPO) and neutrophil elastase (NE). To determine whether the presence of these products correlated with the epithelial damage, we measured the concentration of these products in the apical surface media. We found that the concentration of NE, in apical surface media of the nAEC cultures, was >3 fold greater following neutrophil migration across RSV infected epithelium for 4h (but not 1h) at 72h post infection (**Figure 5AB**) with a mean \pm SEM of $2.0\pm 0.6\text{mU/ml}$, compared to $0.6\pm 0.1\text{mU/ml}$ in the mock-infected cultures ($P=0.039$) (**Figure 5B**). We did not find a significant difference in MPO in apical surface media from RSV infected cultures following neutrophil migration for 1 or 4h compared to the mock-infected cultures ($P=0.0006$)

(**Figure 5CD**). We also did not find a difference in cellular expression of MPO on neutrophils migrated across mock compared to RSV infected epithelium (data not shown).

We found that expression of cellular neutrophil activation marker CD11b was 1.4 fold greater on neutrophils that had migrated across epithelium infected with RSV for 72h (mean (\pm SEM) fluorescence intensity of $1.2 \times 10^4 \pm 1.5 \times 10^3$) compared to $< 8.5 \times 10^3 \pm 4 \times 10^2$ non-migrated neutrophils ($P < 0.05$) (**Figure 5E**), and compared to neutrophils not exposed to the epithelial cells ($5.6 \times 10^3 \pm 1.7 \times 10^3$) ($P < 0.05$). We also found that expression of CD11b was greater on neutrophils that had migrated across RSV infected epithelium after 1h compared to neutrophils that had migrated across mock compared to RSV infected epithelium ($P < 0.05$) (**Figure 5E**).

Neutrophil trans-epithelial migration reduces the infectious viral load

Apical surface media and apical cell layers collected 4h after migration exhibited significantly lower viral titre of 1.6×10^4 pfu/ml in RSV infected ciliated nAEC cultures after neutrophil migration, compared to 4.4×10^5 pfu/ml in RSV infected nAECs without neutrophil migration ($P = 0.03$) (**Figure 5F**). This is a mean \pm SEM difference in viral titre of $-2.7 \times 10^4 \pm 1.2 \times 10^4$ pfu/ml (see supplementary **Figure S6A**). These findings were confirmed by the observation of fewer GFP-positive cells following neutrophil migration from whole well scans (**Figure 5I**) and time-lapse fluorescence microscopy, which showed less GFP expression following neutrophil migration (see **Video3** and **Figure 5H**). There was no significant difference in viral RNA in RSV infected cultures 4h after neutrophil migration (**Figure 5G** and **Figure S6B**). Interestingly, neutrophils exposed to RSV in absence of nAECs also showed a reduction in infectious viral load after 4h, with a difference in viral

titre of $-1.1 \times 10^5 \pm 1.3 \times 10^4$ pfu/ml (see supplementary **Figure S7A**), again there was no difference in viral RNA (supplementary **Figure S7B**).

Blocking neutrophil β 2-integrin lymphocyte function-associated antigen-1 (LFA-1) reduces neutrophil adherence and epithelial damage

We found that ICAM-1 expression was significantly greater on epithelial cells after 72h RSV infection compared with mock-infected epithelial cells ($P < 0.05$) (**Figure S2**) and so we focussed on this time point for these studies. We found fewer neutrophils adhered to RSV infected epithelium when exposed to an inhibitor that blocked the interaction of neutrophil LFA-1 and intercellular cell adhesion molecule 1 (ICAM-1) on epithelial cells compared to the RSV infected epithelium alone ($P < 0.0001$) (**Figure 6A**). We also observed smaller, less frequent neutrophil aggregates when using the LFA-1 inhibitor compared to the RSV infected epithelium (observational data). There was no difference in the number of neutrophils that migrated across the RSV+LFA-1 group compared to the RSV group (**Figure 6B**), suggesting addition of the LFA-1 inhibitor does not affect neutrophil chemotaxis across the epithelium.

We found less epithelial cell shedding and fewer gaps formed in the epithelial layer after 4h when the RSV infected epithelium exposed to the LFA-1 inhibitor (**Figure 6C-E**) compared to the RSV infected epithelium ($P = 0.003$). As before, we did not detect any changes in TEER and red dextran flux in RSV infected epithelium exposed to the LFA-1 inhibitor (**Figure S6**). Interestingly, we found that after 4h neutrophil migration RSV infected epithelium and RSV infected epithelium exposed to the LFA-1 inhibitor both showed higher neutrophil elastase release compared to the mock-infected cells ($P = 0.03$) (**Figure 6F**). In addition, exposure to the LFA-1 inhibitor also reduced viral titre of RSV infected epithelial cells after neutrophil migration ($P = 0.049$) (**Figure 6G**).

Discussion

Here we showed that neutrophil migration and adherence to RSV infected airway epithelial cells was associated with greater epithelial cell damage, greater neutrophil degranulation and a reduction in infectious viral load. We showed that these effects are mediated, at least in part, by the β 2-integrin ligand LFA-1 on neutrophils binding to the ICAM-1 receptor on nAECs, as inhibition of this interaction prevented neutrophil associated epithelial damage.

The airways of infants with RSV bronchiolitis contain a large infiltrate of neutrophils, which have migrated from the bloodstream and across the airway epithelium. There is limited understanding of how this influx of neutrophils contributes to the pathophysiology of RSV infection. Previous studies using *in vitro* human ciliated airway epithelial cell models of RSV infection, while reporting that viral replication within ciliated nAECs peaks in the first 24-72h, by contrast shows little evidence of damage to the epithelial cells during this period of RSV infection [6, 9]. Using this new human airway model to investigate the neutrophil-mediated response in RSV infected ciliated epithelial airway cells and mock infected cells, we have shown for the first time:

- 1) Infection with RSV infected increased the numbers of neutrophils that migrated across the epithelium, after both early and late infection. The presence of apical surface media in the absence of infected cells also achieved this effect after 72 hours. This supports the clinical findings that neutrophil infiltration in the lungs of infants with RSV bronchiolitis [10] correlates with disease severity [15, 28, 29]. Infection of the epithelium with RSV also caused more neutrophils to remain adherent to the epithelium and not detach into the apical surface media. Comparison with mock infected cells exposed to apical surface media from infected cells suggested that this increase in neutrophil adherence was dependent on RSV

infectious particles present in or around the epithelial cells. The adherent neutrophils appeared to form large clusters, suggesting that the neutrophils coordinate or localise their migration. This is a similar finding to that of Yonker *et al* who showed that neutrophil trans-epithelial migration across epithelium infected with *Pseudomonas aeruginosa* led to clumping of neutrophils [30]. Neutrophil swarming has also been observed in other infections and inflammatory diseases [31–33].

2) Neutrophil trans-epithelial migration across differentiated primary human airway epithelium infected with RSV was associated with epithelial damage, including cell shedding and reduced ciliary beat frequency (CBF). We detected an immediate (0-30min) reduction in CBF following neutrophil trans-epithelial migration across ciliated epithelium infected with RSV for 24h. This sensitive readout could be an early indication of cell damage with neutrophil trans-epithelial migration leading rapidly to cilia slowing down. After 4h neutrophil trans-epithelial migration there was an increase in CBF of RSV infected epithelium, back to pre-neutrophil levels. This may indicate that neutrophil migration leads to a loss of the slower beating or damaged cilia, thus explaining the greater average beat frequency of the sampling area after this duration of infection.

3) Epithelial damage was associated with greater neutrophil activation and degranulation, with greater release of neutrophil elastase (NE) into the apical surface media. Neutrophil degranulation is an important feature of the host response and pathophysiology of RSV infection [34, 35]. A previous *in vitro* study demonstrated that RSV stimulated MPO release from neutrophils [36], which is consistent with our findings. The levels of NE, MPO and MMP-9 in sputum and bronchoalveolar lavage fluid have also been shown to correlate with indices of disease severity in airway diseases [37, 38].

4) Loss of epithelial cells and increased LDH release that was specific to RSV infected epithelium. We did not detect a change in TEER. This may be due to the non-migrated neutrophils forming a sediment on the basolateral side of the membrane, which could increase the electrical resistance and compensate for the gaps in apical epithelial cells we detected. Despite the migration of similar numbers of neutrophils towards apical surface media collected from RSV infected cells or the neutrophil chemoattractant fMLP, compared to migration across RSV infected epithelium, this did not lead to epithelial cell shedding or LDH release. This suggests that damage is dependent on the presence of RSV infected epithelial cells. Sloughing off of these infected epithelial cells may lead to obstruction in the small airways of young infants [39]. RSV NS2 protein has been shown to contribute to epithelial shedding and acute airway obstruction in an animal model [11].

We also showed that neutrophil-mediated RSV-induced epithelial damage leads to a reduction in viral load. This antiviral activity could be directly mediated by neutrophils, either by degranulation or by phagocytosis of RSV infected cells, thereby preventing further viral spread. Additional experiments conducted with neutrophils and RSV in absence of infected nAECs supported the findings that neutrophils have an anti-viral effect in that they reduce the amount of infectious particles but not the amount of RNA (**Figure S7**). Some previous studies support this finding and neutrophils have been shown to be beneficial in viral respiratory tract infections [40–42] and are thought to contribute to antiviral defense [43, 44]. However, studies using neutrophil depleted mice concluded that neutrophils were unlikely to play a major role in viral clearance during RSV infection, as viral loads [45] and lung damage [40] were equivalent to those reported in the wild-type mice. We found that neutrophil trans-epithelial migration reduced the amount of infectious RSV, but did not alter the amount of viral RNA recovered from RSV infected ciliated epithelium. This difference

may be due to the sensitivities of the assays with inactivated viral particles present in neutrophils and/or epithelial cells that have intact or partially-fragmented viral RNA.

Since we observed less epithelial damage in conditions where fewer neutrophils adhered, we hypothesised that the neutrophil adherence to the RSV infected epithelium was responsible for the epithelial damage. To investigate this we used an inhibitor that blocked the interaction between LFA-1 on neutrophils and ICAM-1 on nAECs. This inhibitor reduced neutrophil adherence to RSV infected epithelium and considerably reduced epithelial damage, although the number of migrated neutrophils and neutrophil elastase release was unaffected. This suggests that the epithelial damage is mediated by the proximity or direct interaction of neutrophils with RSV infected epithelium. The organisation and clustering of adherent neutrophils could be an important mechanism that drives RSV disease severity. Previous reports have shown that localised LTB₄ signalling is responsible for neutrophil swarming and the coordinated clustering of neutrophils could accelerate neutrophilic inflammation [33]. The accessibility to the cells of interest in our model offers a methodological advantage over *in vivo* and intravital methods and that could allow us to investigate human cellular and transcriptomic changes at a single cell level. Future work by our group aims to compare the transcriptomic and functional behaviour of neutrophils during RSV infection.

To conclude, this study reveals that neutrophil trans-epithelial migration and adherence to epithelial cells quickly results in poorer ciliary function, tissue damage and increased viral killing in RSV infected ciliated cell cultures. Further work to investigate the mechanisms of migration, including neutrophil dynamics, signalling, swarming and activation, could

improve our understanding of the infant immune response in RSV bronchiolitis and help develop new therapeutics.

References

1. Nair H, Nokes DJ, Gessner BD, Dherani M, Madhi SA, Singleton RJ, O'Brien KL, Roca A, Wright PF, Bruce N, Chandran A, Theodoratou E, Sutanto A, Sedyaningsih ER, Ngama M, Munywoki PK, Kartasasmita C, Simões EAF, Rudan I, Weber MW, Campbell H. Global burden of acute lower respiratory infections due to respiratory syncytial virus in young children: a systematic review and meta-analysis. *The Lancet* 2010; 375: 1545–1555.
2. Blanco JCG, Boukhvalova MS, Morrison TG, Vogel SN. A multifaceted approach to RSV vaccination. *Hum Vaccines Immunother* 2018; 14: 1734–1745.
3. DeVincenzo JP, McClure MW, Symons JA, Fathi H, Westland C, Chanda S, Lambkin-Williams R, Smith P, Zhang Q, Beigelman L, Blatt LM, Fry J. Activity of Oral ALS-008176 in a Respiratory Syncytial Virus Challenge Study. *N Engl J Med* 2015; 373: 2048–2058.
4. DeVincenzo JP, Whitley RJ, Mackman RL, Scaglioni-Weinlich C, Harrison L, Farrell E, McBride S, Lambkin-Williams R, Jordan R, Xin Y, Ramanathan S, O'Riordan T, Lewis SA, Li X, Toback SL, Lin S-L, Chien JW. Oral GS-5806 activity in a respiratory syncytial virus challenge study. *N Engl J Med* 2014; 371: 711–722.
5. Stevens M, Rusch S, DeVincenzo J, Kim Y-I, Harrison L, Meals EA, Boyers A, Fok-Seang J, Huntjens D, Lounis N, Mari N K, Remmerie B, Roymans D, Koul A, Verloes R. Antiviral Activity of Oral JNJ-53718678 in Healthy Adult Volunteers Challenged With Respiratory Syncytial Virus: A Placebo-Controlled Study. *J Infect Dis* 2018; 218: 748–756.
6. Villenave R, Thavagnanam S, Sarlang S, Parker J, Douglas I, Skibinski G, Heaney LG, McKaigue JP, Coyle PV, Shields MD, Power UF. In vitro modeling of respiratory syncytial virus infection of pediatric bronchial epithelium, the primary target of infection in vivo. *Proc Natl Acad Sci U S A* 2012; 109: 5040–5045.
7. Tristram DA, Hicks W, Hard R. Respiratory syncytial virus and human bronchial epithelium. *Arch Otolaryngol Head Neck Surg* 1998; 124: 777–783.
8. Zhang L, Peeples ME, Boucher RC, Collins PL, Pickles RJ. Respiratory syncytial virus infection of human airway epithelial cells is polarized, specific to ciliated cells, and without obvious cytopathology. *J Virol* 2002; 76: 5654–5666.
9. Smith CM, Kulkarni H, Radhakrishnan P, Rutman A, Bankart MJ, Williams G, Hirst RA, Easton AJ, Andrew PW, O'Callaghan C. Ciliary dyskinesia is an early feature of respiratory syncytial virus infection. *Eur Respir J* 2014; 43: 485–496.
10. Welliver TP, Garofalo RP, Hosakote Y, Hintz KH, Avendano L, Sanchez K, Velozo L, Jafri H, Chavez-Bueno S, Ogra PL, McKinney L, Reed JL, Welliver RC. Severe human lower respiratory tract illness caused by respiratory syncytial virus and influenza virus is characterized by the absence of pulmonary cytotoxic lymphocyte responses. *J Infect Dis* 2007; 195: 1126–1136.

11. Liesman RM, Buchholz UJ, Luongo CL, Yang L, Proia AD, DeVincenzo JP, Collins PL, Pickles RJ. RSV-encoded NS2 promotes epithelial cell shedding and distal airway obstruction. *J Clin Invest* 2014; 124: 2219–2233.
12. McNamara PS, Ritson P, Selby A, Hart CA, Smyth RL. Bronchoalveolar lavage cellularity in infants with severe respiratory syncytial virus bronchiolitis. *Arch Dis Child* 2003; 88: 922–926.
13. Everard ML, Swarbrick A, Wraitham M, McIntyre J, Dunkley C, James PD, Sewell HF, Milner AD. Analysis of cells obtained by bronchial lavage of infants with respiratory syncytial virus infection. *Arch Dis Child* 1994; 71: 428–432.
14. Deng Y, Herbert JA, Smith CM, Smyth RL. An in vitro transepithelial migration assay to evaluate the role of neutrophils in Respiratory Syncytial Virus (RSV) induced epithelial damage. *Sci Rep* 2018; 8: 6777.
15. Wang SZ, Xu H, Wraith A, Bowden JJ, Alpers JH, Forsyth KD. Neutrophils induce damage to respiratory epithelial cells infected with respiratory syncytial virus. *Eur Respir J* 1998; 12: 612–618.
16. Stark J M, Godding V, Sedgwick J B, Busse W W. intercellular adhesion molecule-1.respiratory epithelial cells. Roles of CD18 and intercellular adhesion molecule-1. . *The Journal of Immunology* 1996; .
17. Hosakote YM, Brasier AR, Casola A, Garofalo RP, Kurosky A. Respiratory Syncytial Virus Infection Triggers Epithelial HMGB1 Release as a Damage-Associated Molecular Pattern Promoting a Monocytic Inflammatory Response. *J Virol* 2016; 90: 9618–9631.
18. Fix J, Galloux M, Blondot M-L, Eléouët J-F. The insertion of fluorescent proteins in a variable region of respiratory syncytial virus L polymerase results in fluorescent and functional enzymes but with reduced activities. *Open Virol J* 2011; 5: 103–108.
19. Dewhurst-Maridor G, Simonet V, Bornand JE, Nicod LP, Pache JC. Development of a quantitative TaqMan RT-PCR for respiratory syncytial virus. *J Virol Methods* 2004; 120: 41–49.
20. Castagné N, Barbier A, Bernard J, Rezaei H, Huet J-C, Henry C, Da Costa B, Eléouët J-F. Biochemical characterization of the respiratory syncytial virus P-P and P-N protein complexes and localization of the P protein oligomerization domain. *J Gen Virol* 2004; 85: 1643–1653.
21. Chilvers MA, O’Callaghan C. Analysis of ciliary beat pattern and beat frequency using digital high speed imaging: comparison with the photomultiplier and photodiode methods. *Thorax* 2000; 55: 314–317.
22. Butler CR, Hynds RE, Gowers KHC, Lee DDH, Brown JM, Crowley C, Teixeira VH, Smith CM, Urbani L, Hamilton NJ, Thakrar RM, Booth HL, Birchall MA, De Coppi P, Giangreco A, O’Callaghan C, Janes SM. Rapid expansion of human epithelial stem

- cells suitable for airway tissue engineering. *Am J Respir Crit Care Med* 2016; 194: 156–168.
23. Winn M, Reilly EB, Liu G, Huth JR, Jae HS, Freeman J, Pei Z, Xin Z, Lynch J, Kester J, Geldern TW von, Leitz S, DeVries P, Dickinson R, Mussatto D, Okasinski GF. Discovery of novel p-arylthio cinnamides as antagonists of leukocyte function-associated antigen-1/intercellular adhesion molecule-1 interaction. 4. Structure-activity relationship of substituents on the benzene ring of the cinnamide. *J Med Chem* 2001; 44: 4393–4403.
 24. Liu G, Link JT, Pei Z, Reilly EB, Leitz S, Nguyen B, Marsh KC, Okasinski GF, Geldern TW von, Ormes M, Fowler K, Gallatin M. Discovery of Novel p -Arylthio Cinnamides as Antagonists of Leukocyte Function-Associated Antigen-1/Intracellular Adhesion Molecule-1 Interaction. 1. Identification of an Additional Binding Pocket Based on an Anilino Diaryl Sulfide Lead. *J Med Chem* 2000; 43: 4025–4040.
 25. Keating SM, Clark KR, Stefanich LD, Arellano F, Edwards CP, Bodary SC, Spencer SA, Gadek TR, Marsters JC, Beresini MH. Competition between intercellular adhesion molecule-1 and a small-molecule antagonist for a common binding site on the alpha subunit of lymphocyte function-associated antigen-1. *Protein Sci* 2006; 15: 290–303.
 26. Smith CM, Djakow J, Free RC, Djakow P, Lonnen R, Williams G, Pohunek P, Hirst RA, Easton AJ, Andrew PW, O’Callaghan C. ciliaFA: a research tool for automated, high-throughput measurement of ciliary beat frequency using freely available software. *Cilia* 2012; 1: 14.
 27. Thomas B, Aurora P, Spencer H, Elliott M, Rutman A, Hirst RA, O’Callaghan C. Persistent disruption of ciliated epithelium following paediatric lung transplantation. *Eur Respir J* 2012; 40: 1245–1252.
 28. Yasui K, Baba A, Iwasaki Y, Kubo T, Aoyama K, Mori T, Yamazaki T, Kobayashi N, Ishiguro A. Neutrophil-mediated inflammation in respiratory syncytial viral bronchiolitis. *Pediatr Int* 2005; 47: 190–195.
 29. Jones A, Qui JM, Bataki E, Elphick H, Ritson S, Evans GS, Everard ML. Neutrophil survival is prolonged in the airways of healthy infants and infants with RSV bronchiolitis. *Eur Respir J* 2002; 20: 651–657.
 30. Yonker LM, Mou H, Chu KK, Pazos MA, Leung H, Cui D, Ryu J, Hibbler RM, Eaton AD, Ford TN, Falck JR, Kinane TB, Tearney GJ, Rajagopal J, Hurley BP. Development of a Primary Human Co-Culture Model of Inflamed Airway Mucosa. *Sci Rep* 2017; 7: 8182.
 31. Peters NC, Egen JG, Secundino N, Debrabant A, Kimblin N, Kamhawi S, Lawyer P, Fay MP, Germain RN, Sacks D. In vivo imaging reveals an essential role for neutrophils in leishmaniasis transmitted by sand flies. *Science* 2008; 321: 970–974.
 32. McDonald B, Pittman K, Menezes GB, Hirota SA, Slaba I, Waterhouse CCM, Beck PL, Muruve DA, Kubes P. Intravascular danger signals guide neutrophils to sites of sterile inflammation. *Science* 2010; 330: 362–366.

33. Lämmermann T, Afonso PV, Angermann BR, Wang JM, Kastenmüller W, Parent CA, Germain RN. Neutrophil swarms require LTB₄ and integrins at sites of cell death in vivo. *Nature* 2013; 498: 371–375.
34. Darville T, Yamauchi T. Respiratory syncytial virus. *Pediatr Rev* 1998; 19: 55–61.
35. Lundgren JD, Rieves RD, Mullol J, Logun C, Shelhamer JH. The effect of neutrophil proteinase enzymes on the release of mucus from feline and human airway cultures. *Respir Med* 1994; 88: 511–518.
36. Jaovisidha P, Peeples ME, Brees AA, Carpenter LR, Moy JN. Respiratory syncytial virus stimulates neutrophil degranulation and chemokine release. *J Immunol* 1999; 163: 2816–2820.
37. Garratt LW, Sutanto EN, Ling K-M, Looi K, Iosifidis T, Martinovich KM, Shaw NC, Kicic-Starcevic E, Knight DA, Ranganathan S, Stick SM, Kicic A, Australian Respiratory Early Surveillance Team for Cystic Fibrosis (AREST CF). Matrix metalloproteinase activation by free neutrophil elastase contributes to bronchiectasis progression in early cystic fibrosis. *Eur Respir J* 2015; 46: 384–394.
38. Hoenderdos K, Condliffe A. The neutrophil in chronic obstructive pulmonary disease. Too little, too late or too much, too soon? *atsjournals.org*.
39. Johnson JE, Gonzales RA, Olson SJ, Wright PF, Graham BS. The histopathology of fatal untreated human respiratory syncytial virus infection. *Mod Pathol* 2007; 20: 108–119.
40. Tate MD, Deng Y-M, Jones JE, Anderson GP, Brooks AG, Reading PC. Neutrophils ameliorate lung injury and the development of severe disease during influenza infection. *J Immunol* 2009; 183: 7441–7450.
41. Dienz O, Rud JG, Eaton SM, Lanthier PA, Burg E, Drew A, Bunn J, Suratt BT, Haynes L, Rincon M. Essential role of IL-6 in protection against H1N1 influenza virus by promoting neutrophil survival in the lung. *Mucosal Immunol* 2012; 5: 258–266.
42. Tate MD, Brooks AG, Reading PC, Mintern JD. Neutrophils sustain effective CD8(+) T-cell responses in the respiratory tract following influenza infection. *Immunol Cell Biol* 2012; 90: 197–205.
43. Jenne CN, Kubes P. Virus-induced NETs--critical component of host defense or pathogenic mediator? *PLoS Pathog* 2015; 11: e1004546.
44. Drescher B, Bai F. Neutrophil in viral infections, friend or foe? *Virus Res* 2013; 171: 1–7.
45. Stokes KL, Currier MG, Sakamoto K, Lee S, Collins PL, Plemper RK, Moore ML. The respiratory syncytial virus fusion protein and neutrophils mediate the airway mucin response to pathogenic respiratory syncytial virus infection. *J Virol* 2013; 87: 10070–10082.

Acknowledgments:

Funding: YD and LR were recipients of a Newton fellowship from The Academy of Medical Science (ref 0403 and NIF004/1012 respectively). CMS was a recipient of a grant from Wellcome Trust (212516/Z/18/Z). RLS was supported by the Great Ormond Street Children's Charity (grant code W1802). This research was supported by the NIHR Great Ormond Street Hospital Biomedical Research Centre. Microscopy was performed at the Light Microscopy Core Facility, UCL GOS Institute of Child Health supported by the NIHR GOSH BRC award 17DD08. The views expressed are those of the author(s) and not necessarily those of the NHS, the NIHR or the Department of Health.

Author contributions: JAH developed and optimised the inverted neutrophil migration model using primary AEC from nasal brushings, contributed to study design, acquisition and analysis of data, and assembly of the manuscript. YD contributed to study design, acquisition and analysis of data, and assembly of the manuscript. PH contributed to statistical analysis of the data. LR contributed to acquisition and analysis of data, and assembly of the manuscript. ER contributed to acquisition and analysis of data, and review of the manuscript. DM contributed to acquisition and analysis of data, and review of the manuscript. RLS contributed to conception of the study, analysis of the data, assembly and final approval of the manuscript. CMS conceived the study, contributed to study design, analysis of the data, assembly and final approval of the manuscript.

Competing interests: the authors declare no competing interests

Data and materials availability: Raw data files will be made available on Figshare on acceptance of manuscript.

Figure Legends

Figure 1 Schematic diagram of primary human nAEC neutrophil migration model. (1) primary nasal airway epithelial basal cells were seeded onto the underside of a 3µm pore size PET ThinCert membrane inserts and allowed to attach for 4 hours. Membrane inserts were subsequently inverted and maintained in media to allow a confluent epithelial monolayer to develop for 1 day. (2) membrane inserts exposed to an air-liquid interface and allowed to fully differentiate for 28 days (3) membrane inserts were inverted and infected apically with GFP RSV or mock infected for 2 hours and the infection allowed to progress for 24 or 72 hours. (4) Ultrapure neutrophils isolated from venous blood were added to the basolateral side of the membrane inserts, and were allowed to migrate for 1 or 4 hours. Outcome measures are identified.

Figure 2 RSV increases the numbers of neutrophils that migrate across infected nasal epithelial cell cultures (A) The numbers of apical neutrophils that migrated across RSV infected airway epithelial cell cultures and are released into the apical surface media after 24h infection (B) The numbers of apical neutrophils that migrated across RSV infected airway epithelial cell cultures and are released into the apical surface media after 72h infection. For all bars show mean \pm SEM of n= 6 epithelial donors, 6 heterologous blood donors. (C) The number of neutrophils attached to mock or respiratory syncytial virus (RSV)-infected human nasal ciliated epithelial cells after 24 infection. (D) The number of neutrophils attached to mock or respiratory syncytial virus (RSV)-infected human nasal ciliated epithelial cells after 72 infection. Neutrophil concentrations were quantified in the apical surface media using plate reader and read against a standard curve. Adhered neutrophils were counted using ImageJ counting tool, the average number of neutrophils from all images is shown (5 images

per well from n=3 epithelial donors, 2 heterologous and 1 homologous blood donors). Bars represent the mean \pm SEM for cultures mock infected (white bars), RSV infected (black bars), mock infected and exposed to apical surface media collected from RSV infected cells (checkered bars) or mock infected and exposed apically to the chemoattractant fMLP (striped bars). Statistical comparison between all groups was performed using a paired t-test. Statistical significance is shown

Figure 3 Neutrophil trans-epithelial migration increases the damage caused to RSV

infected ciliated epithelium (A) Representative confocal images of respiratory syncytial virus (RSV)-infected human nasal ciliated epithelial cells grown at an air–liquid interface following neutrophil (red) trans-epithelial migration for 1 or 4 hours. Cells were stained with antibodies against acetylated tubulin to detect the ciliary microtubules (white) and nuclei were stained using Hoescht (blue). Gaps in the epithelial layers can be seen by large ($>500\mu\text{m}^2$) black areas. **(B)** Gap analysis **(C)** The number of epithelial cells attached to membrane inserts after 72h rgRSV infection and 1 and 4 hours after neutrophil migration. Epithelial cells were quantified by counting the DAPI stained nuclei $>50\mu\text{m}^2$ in area using ImageJ. Bars represent the mean \pm SEM for n=5 images per well, 3 epithelial donors, 2 heterologous and 1 autologous blood donors. **(D)** Lactate dehydrogenase (LDH) release was measured in apical surface media of nAECs post neutrophil migration for 1 and 4 hours. Bars represent the mean \pm SEM for n=4 epithelial donors, 3 heterologous and 1 homologous blood donors. **(E)** Trans-epithelial electrical resistance (TEER) of each well as measured using a voltohmmeter, data is represented as the mean \pm SEM of n=4 epithelial donors, 3 heterologous and 1 homologous blood donors. Mock infected (white bars), RSV infected (black bars), mock infected and exposed to apical surface media collected from RSV infected

cells (checkered bars) or mock infected and exposed apically to the chemoattractant fMLP (striped bars). Statistical significance is shown.

Figure 4 The effect of respiratory syncytial virus (RSV) and neutrophil trans-epithelial migration on ciliary beat frequency of human ciliated epithelial cells infected with mock or RSV A2 for 24h (A) or 72h (B) as determined using fast Fourier transformation of high speed video microscopy videos by ciliaFA. Bars represent the mean \pm SEM of n=12 areas per well for cultures mock infected (blue bars), mock infected following neutrophil trans-epithelial migration, RSV infected (red bars), or RSV infected following neutrophil trans-epithelial migration. Statistical comparison between all groups was performed using a paired t-test. n=3 epithelial donors, 3 heterologous blood donors. Statistical significance is shown. (C) Representative Histograms of the frequency distribution of ciliary beat frequency from 1600 regions of interest taken from a representative field of view.

Figure 5 – Release of neutrophil derived products and neutrophil activation after trans-epithelial migration across RSV infected ciliated epithelial cells. Levels of (A/B) neutrophil elastase (NE) and (C/D) myeloperoxidase (MPO) were measured in apical surface medias after migration across mock or RSV infected (24h/ 72h infection) ciliated epithelial monolayers following neutrophil migration for 1 and 4 hour. For all, bars show mean \pm SEM of n = n=4 epithelial donors, 3 heterologous and 1 homologous blood donors. Statistical comparison between all groups was performed using a paired t-test. Statistical significance is shown. (E) Cell surface expression of CD11B is increased on neutrophils that migrated across RSV infected epithelial cells infected for 72 hours show compared to non-migrated neutrophils. The percentage of migrated (M) and non-migrated (NM) neutrophils expressing CD11B was calculated by staining for cell surface expression of CD11B (PE) were

determined by flow cytometry. Neutrophils were gated on initially using a PE positive gate. Using this population the geometric mean fluorescence intensity of PE fluorescence was calculated. Bars show mean \pm SEM of n = 3 epithelial donors, 3 heterologous blood donors. Statistical significance is shown. *P<0.05. **(F/G)** Viral titre at 72h post infection as determined by plaque assay (pfu/ml) (F) or qRT-PCR (G) of whole well lysates showing a decrease in infectious RSV 4h post neutrophil migration. n=10 technical repeats from 6 epithelial donors, 5 heterologous and 1 homologous blood donors **(H)** Time-lapse fluorescence microscopy showing elimination of GFP+ (green) epithelial cell within 50 minutes of the addition of neutrophils (red) to the basolateral side of the epithelial cells. This is also shown in Video 3 **(I)** Whole well fluorescence microscopy scan of a representative membrane insert infected with RSV for 72h cells before (left) and 4h after (right) neutrophil migration. Each white spot indicates an RSV infected epithelial cell. **(I)** Whole well scans using fluorescence microscopy showing the effect of neutrophil migration on overall numbers of RSV infected epithelial cells (RSV+ve cells = green).

Figure 6 – Blocking neutrophil β 2-integrin leukocyte function-associated antigen-1F (LFA1) reduces neutrophil adherence and epithelial damage. **(A)** Number of neutrophils attached to membrane insert 72 hours RSV infection and post migration for 1 and 4 hour were quantified with or without addition of an LFA1 inhibitor. Neutrophils were counted using ImageJ, the average number of neutrophils from all images is shown (5 after 24 and images per donor, n=3 epithelial donors, 2 heterologous and 1 homologous blood donors). **(B)** Numbers of neutrophils that migrated across RSV infected ciliated cell monolayers after 24 and 72 hours RSV infection were quantified with or without addition of an LFA1 inhibitor. LFA1 group is a RSV infected membrane insert with the LFA1 blocker added to the apical surface media collected from RSV infected cells underneath (apical). **(C)** Representative

microscopy images of ciliated epithelial monolayers RSV infected for 24 and 72 hours, stained with a nuclei stain (Hoechst) following neutrophil (red) migration for 1 and 4 hour with or without addition of an LFA1 inhibitor are shown. **(D)** Numbers of epithelial cells attached to membrane insert were quantified after neutrophil migration for 1 and 4 hours in RSV infected groups with or without addition of an LFA1 inhibitor. Epithelial cells were counted using ImageJ, the average number of epithelial cells from all images is shown (5 images per donor, n=3 epithelial donors, 2 heterologous and 1 homologous blood donors). **(E)** Lactate dehydrogenase (LDH) release was measured in apical surface media of AECs post neutrophil migration for 1 and 4 hours in RSV infected groups with or without addition of an LFA1 inhibitor. **(F)** neutrophil elastase (NE) were measured in apical surface medias after migration across 72h RSV infected ciliated epithelial monolayers with and without LFA-1 inhibitor following neutrophil migration for 4 hour. n=2 epithelial donors, 1 heterologous and 1 homologous blood donors **(G)** Viral titre as determined by plaque assay (pfu/ml) of whole well lysates showing a decrease in infectious RSV 4h post neutrophil migration (n=9 technical repeats from 6 epithelial donors, 5 heterologous and 1 homologous blood donors). Statistical significance is shown.

Figure 1

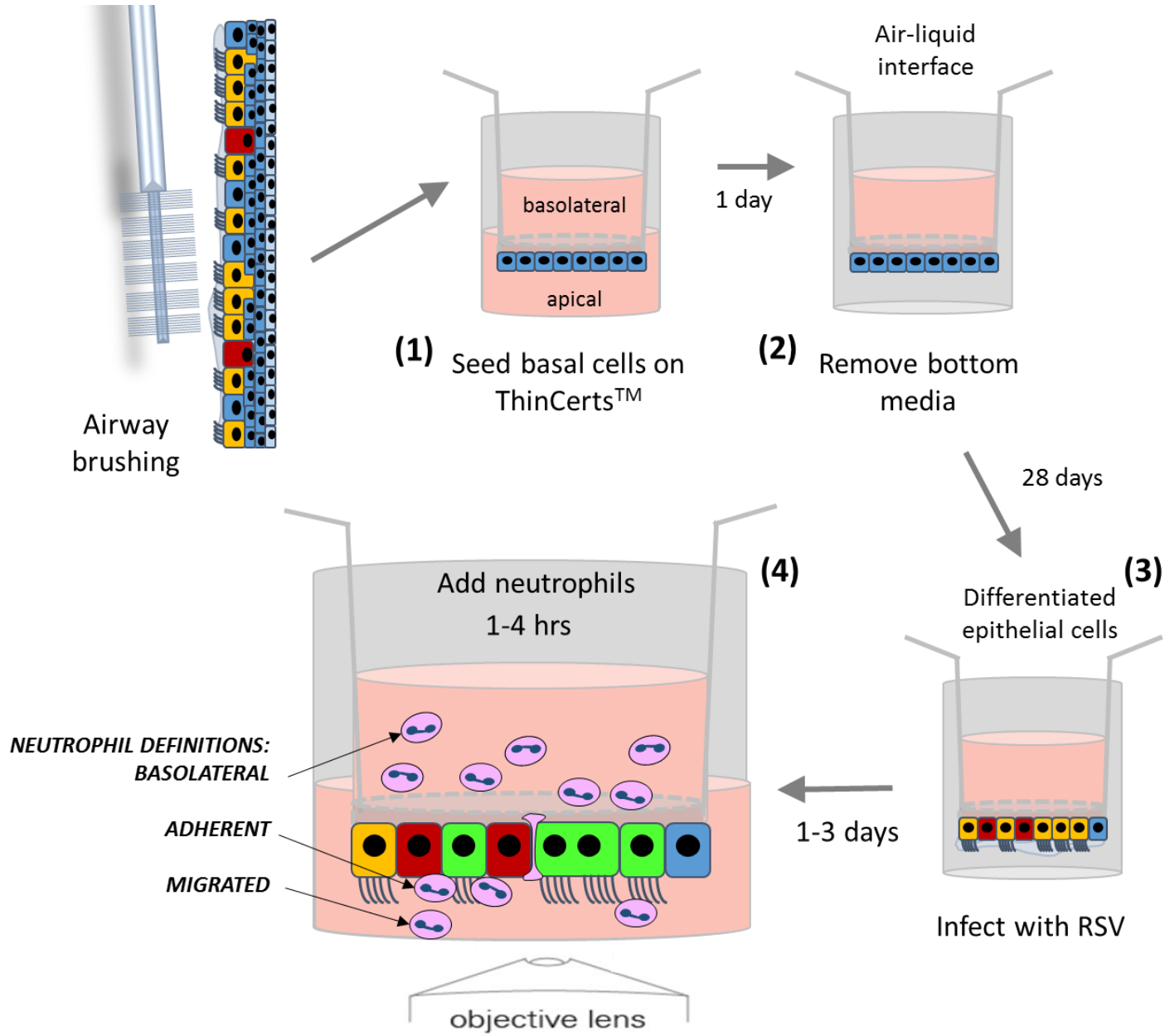


Figure 2

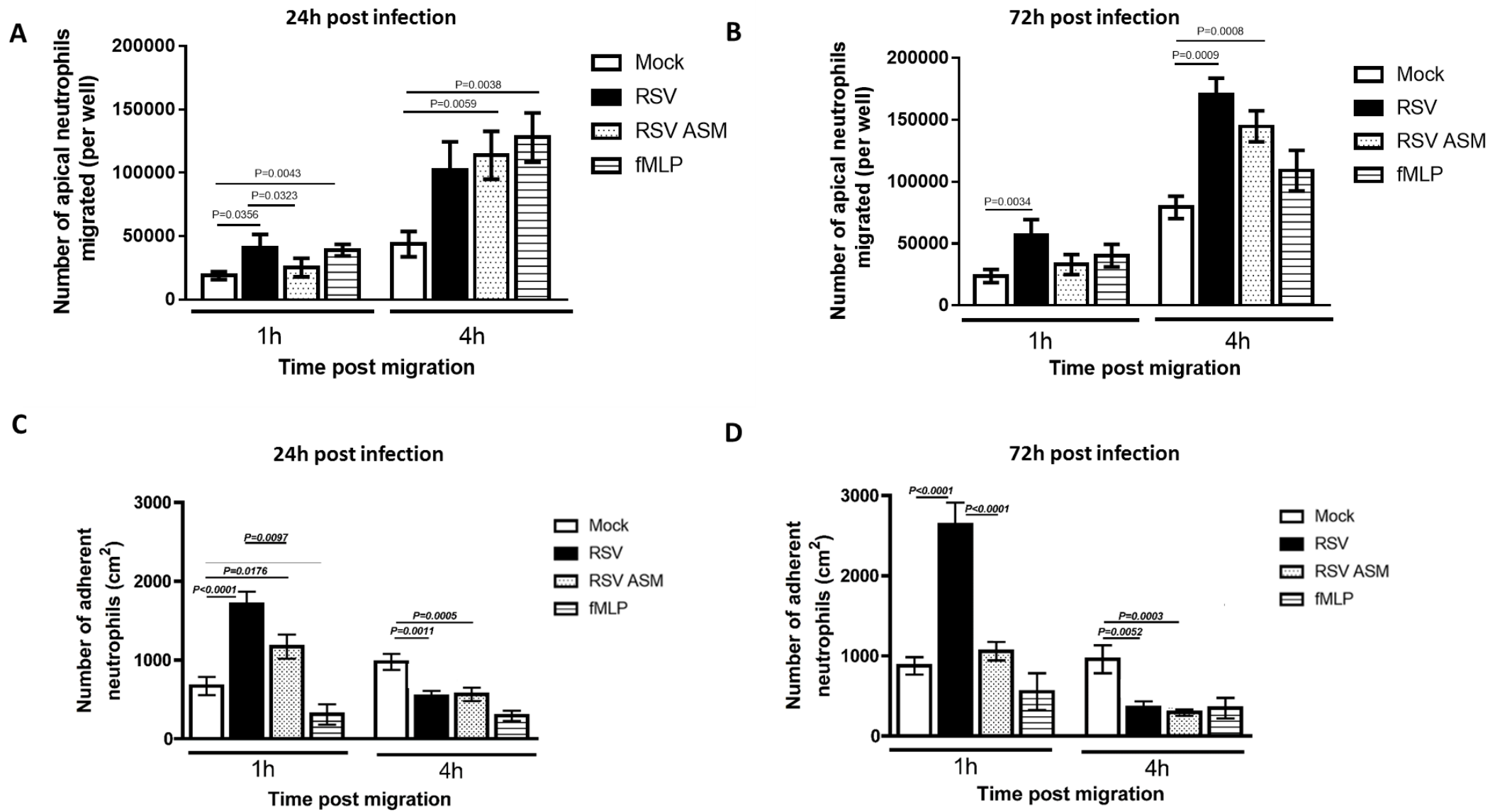
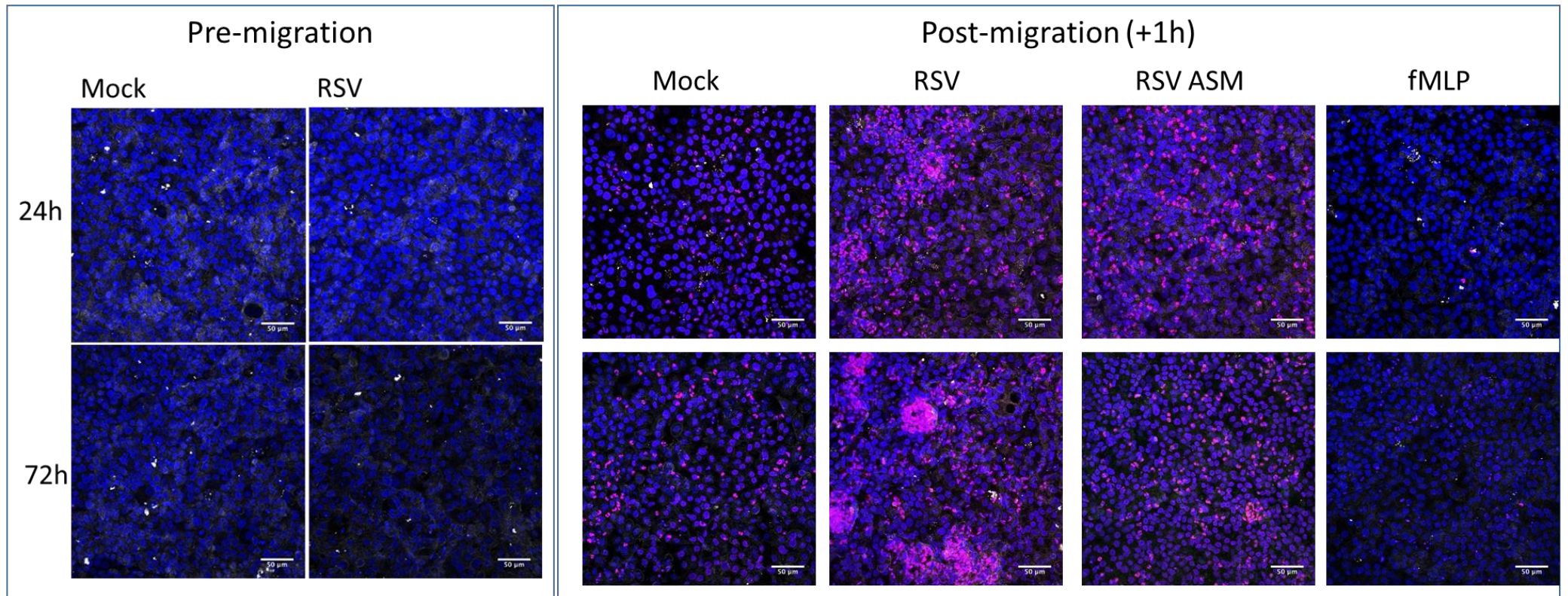


Figure 3

A



A continued...

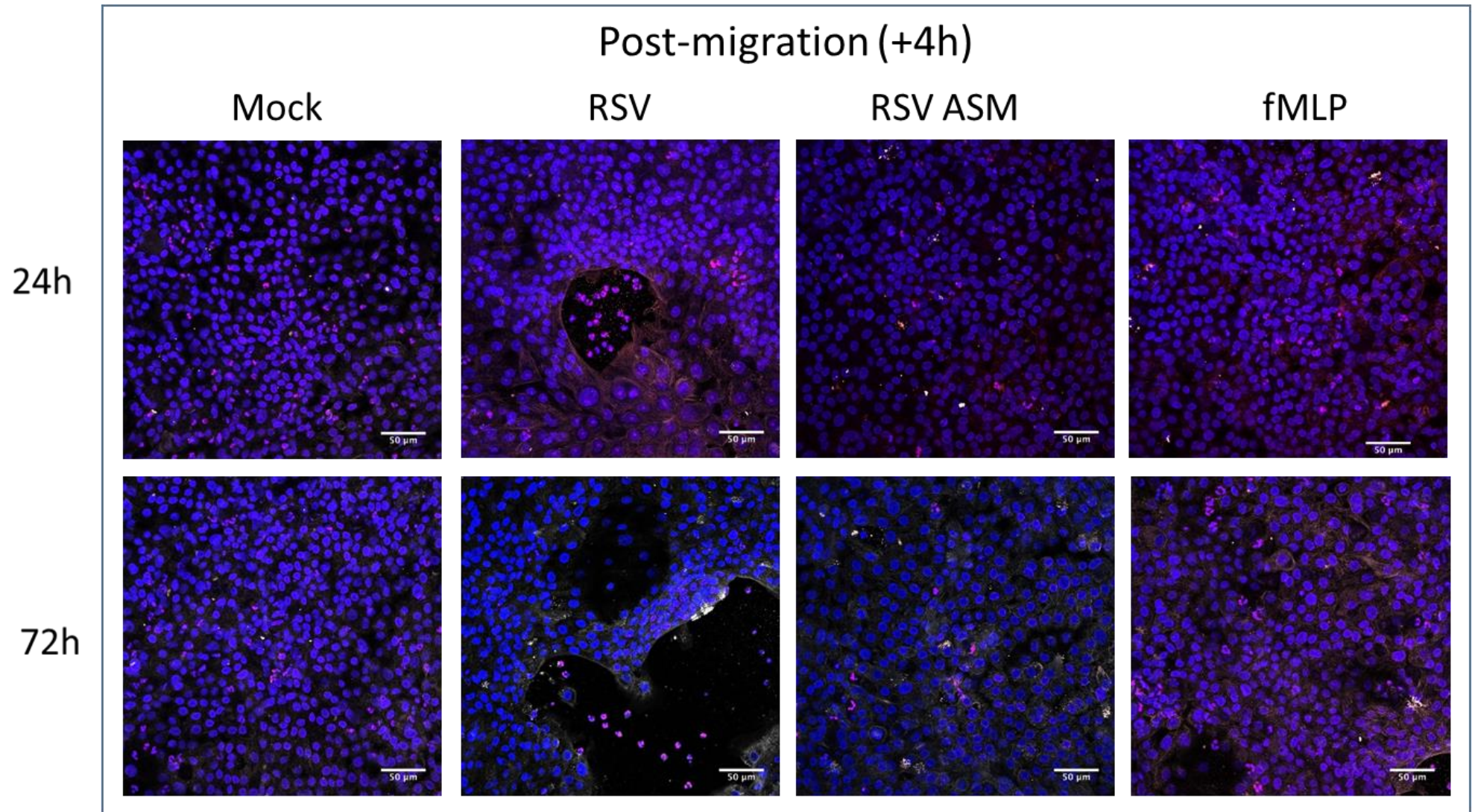
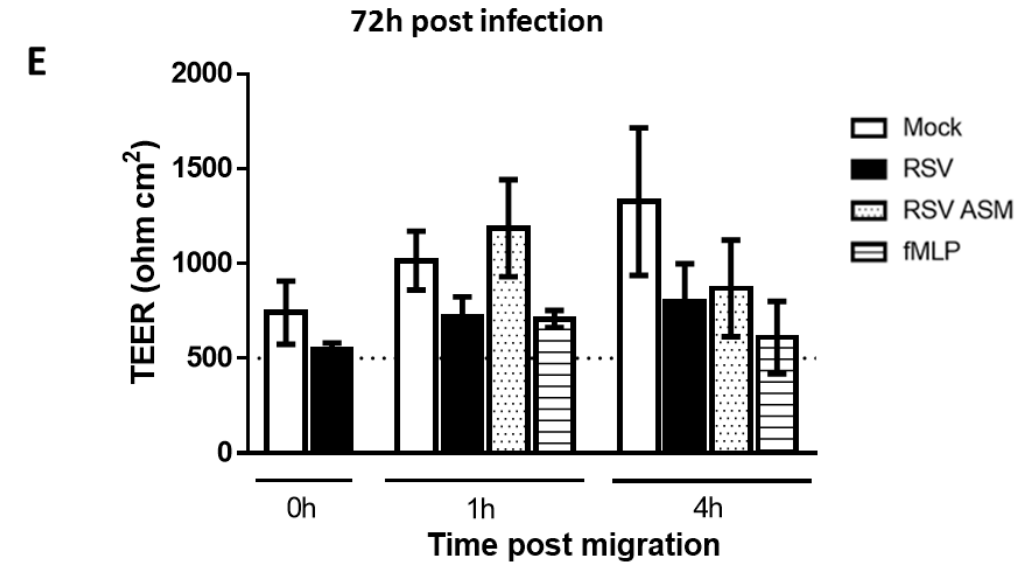
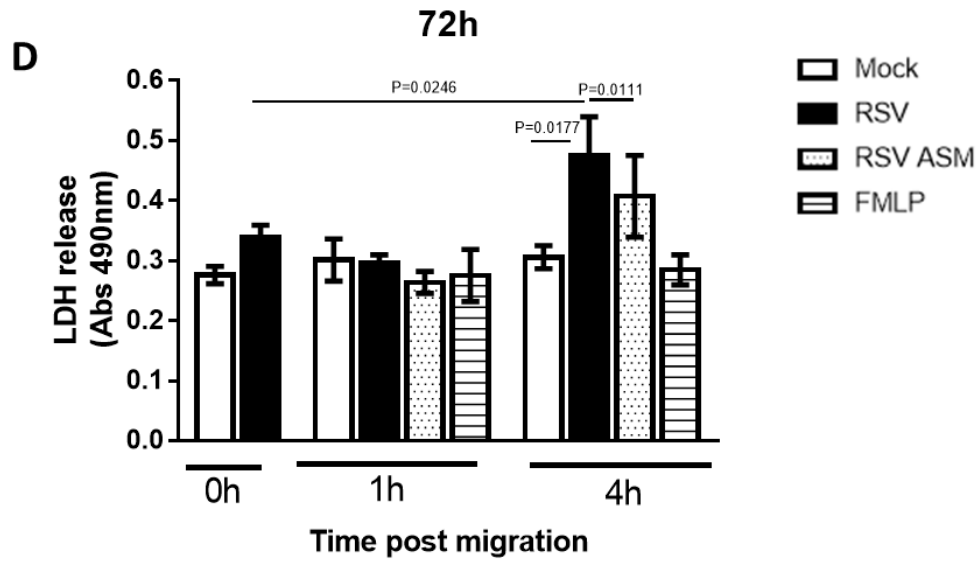
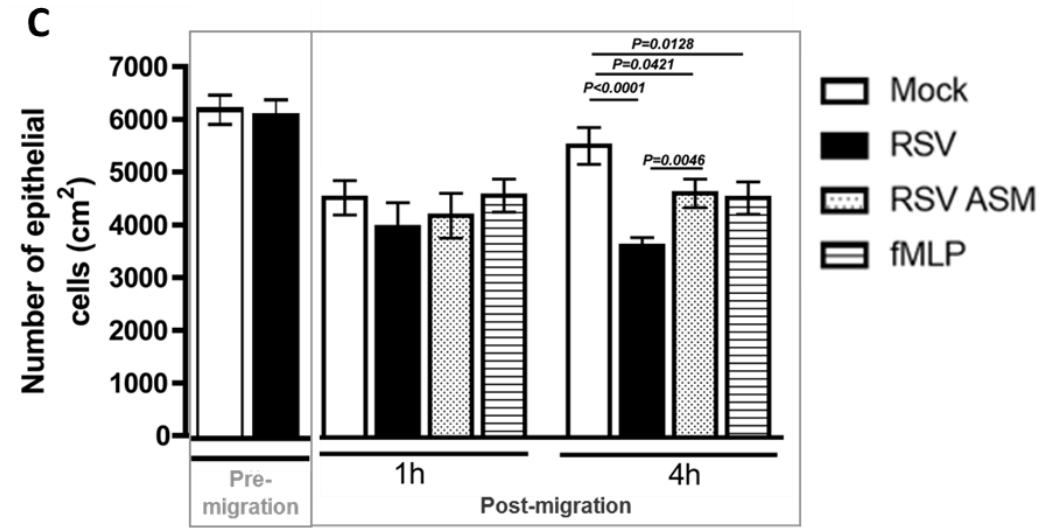
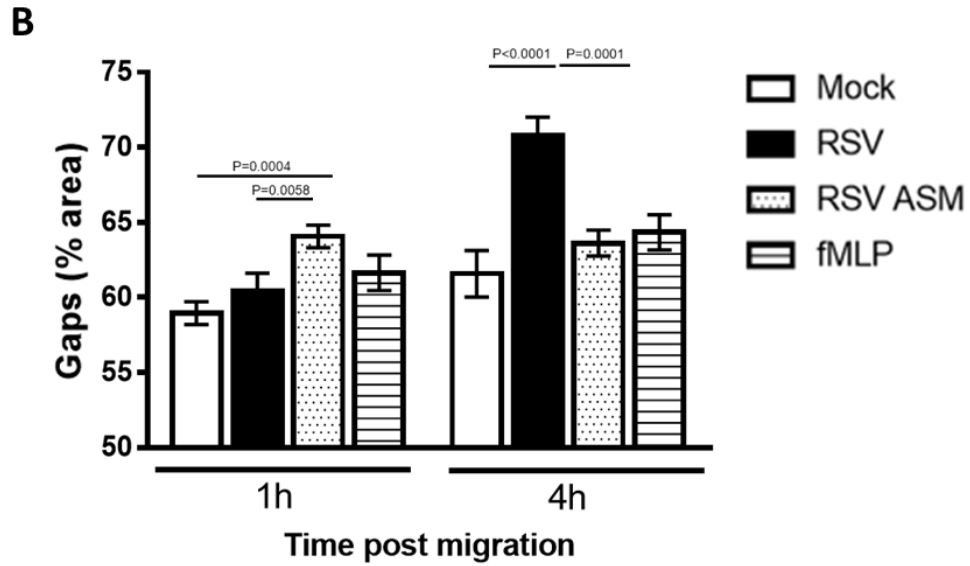


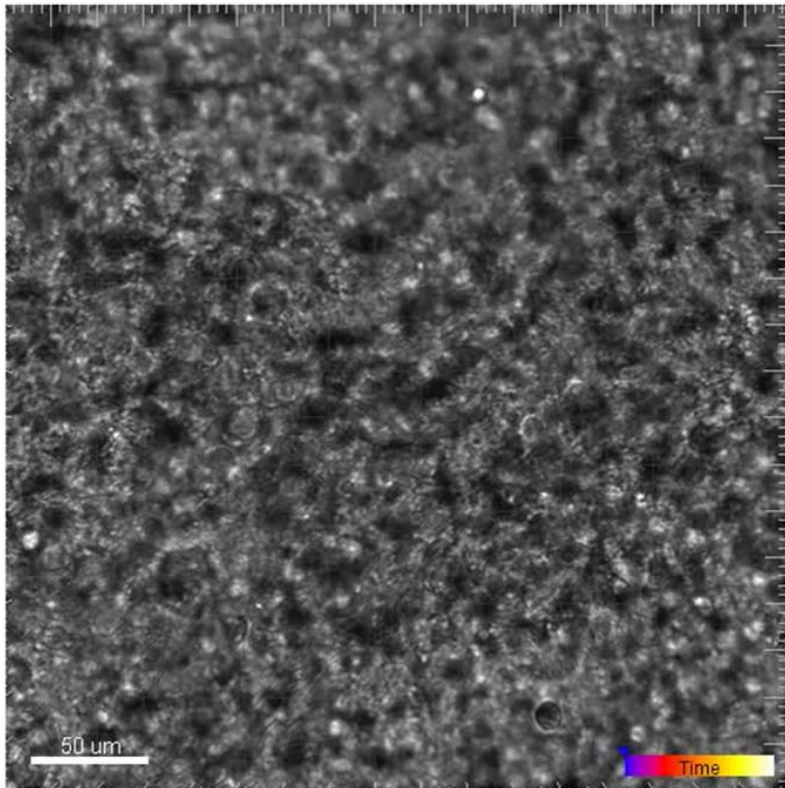
Figure 3



Video 2

Time-lapse video showing epithelial rounding of human ciliated epithelial cells infected with RSV A2 for 72h following neutrophil migration over a 24h period. Images were captured every 30 minutes for 4h then every hour up to 24 hours post neutrophil migration. Scale bar = 50um.

Start frame



End frame

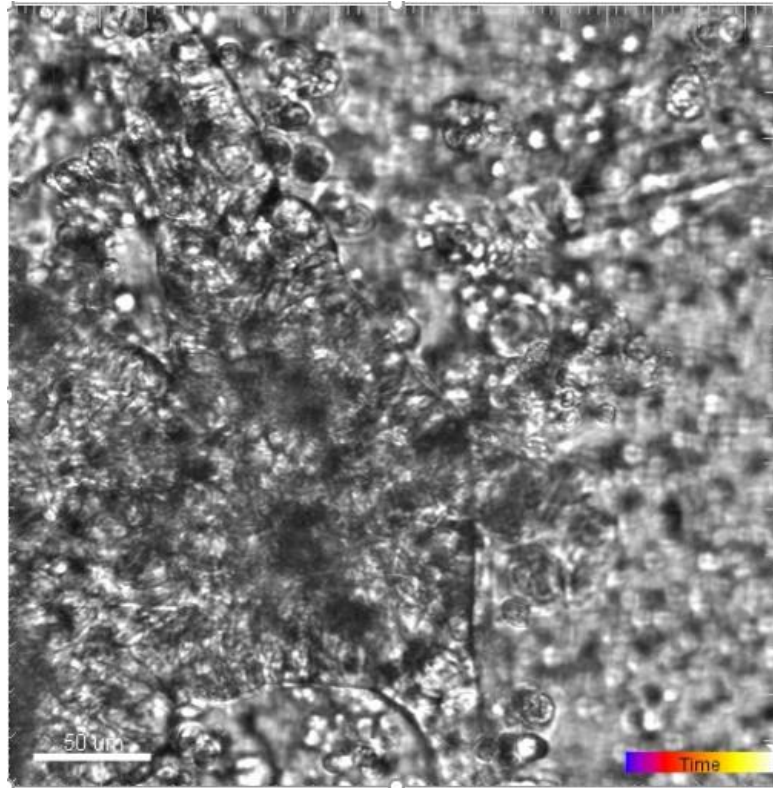
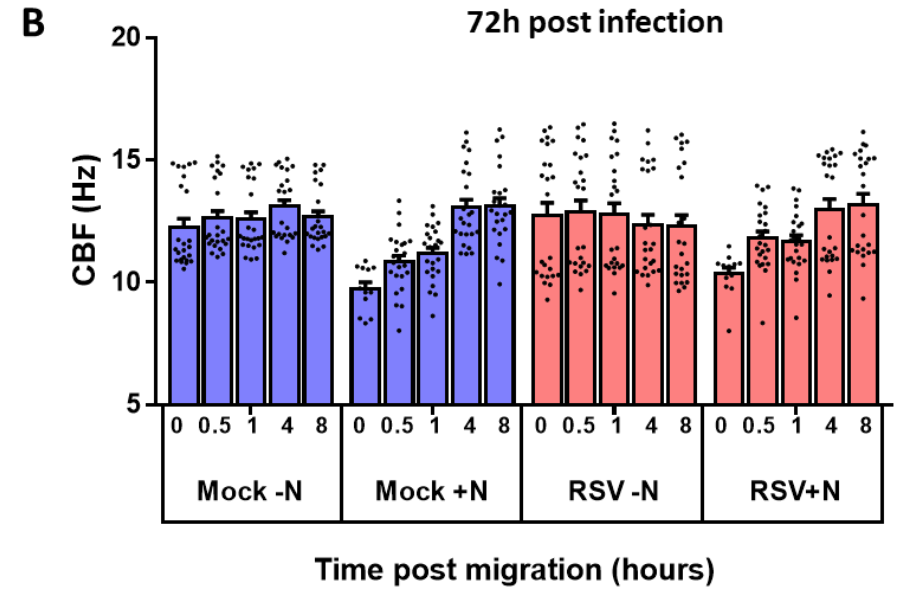
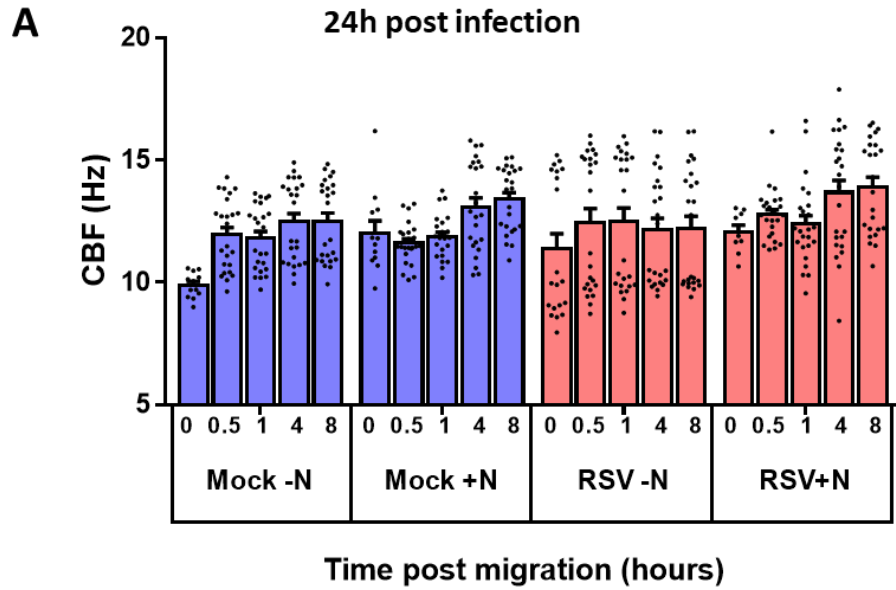


Figure 4



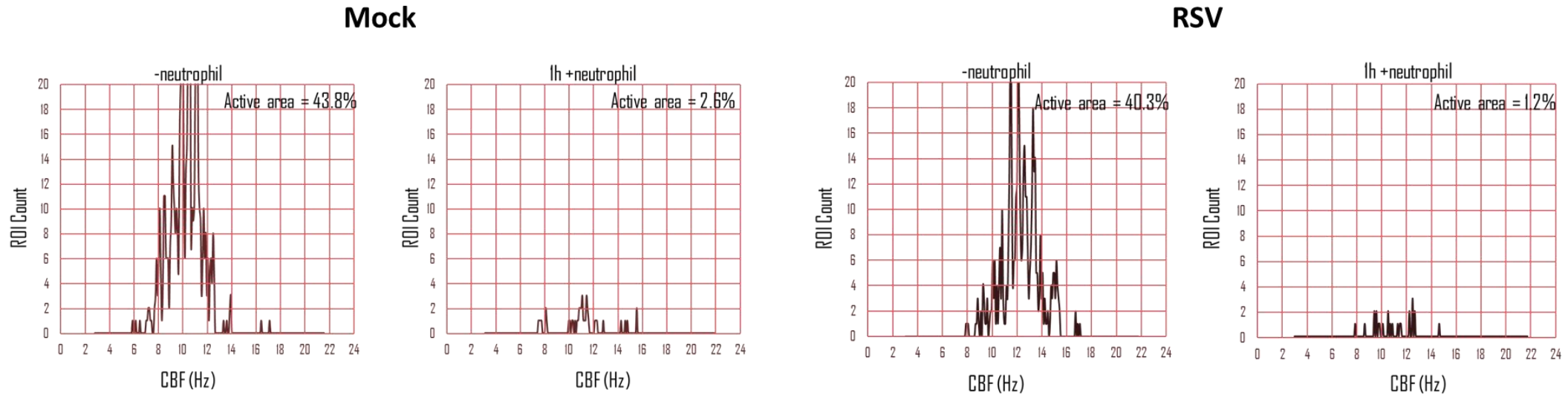
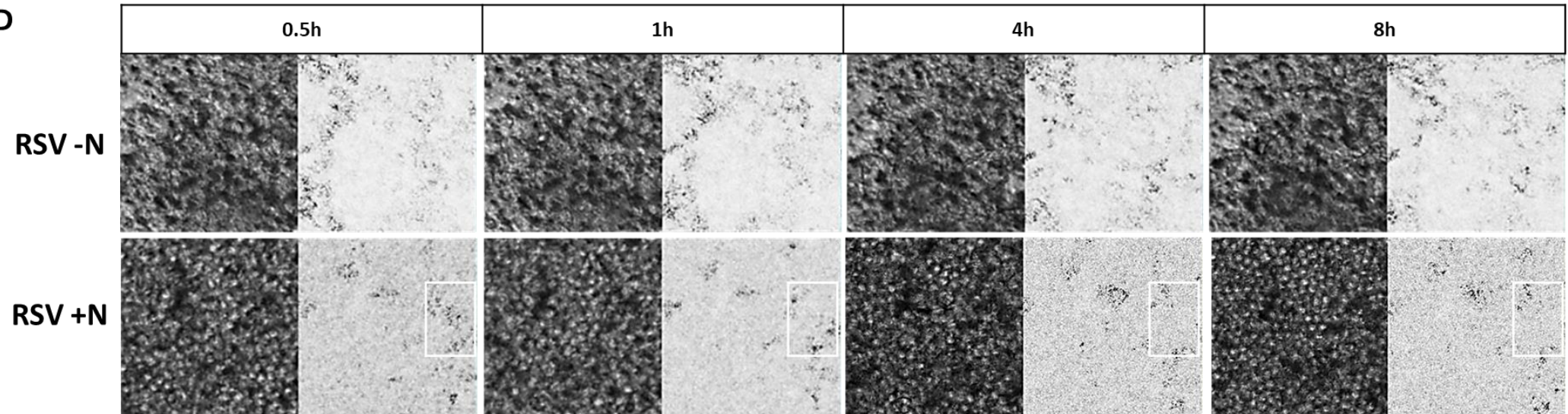
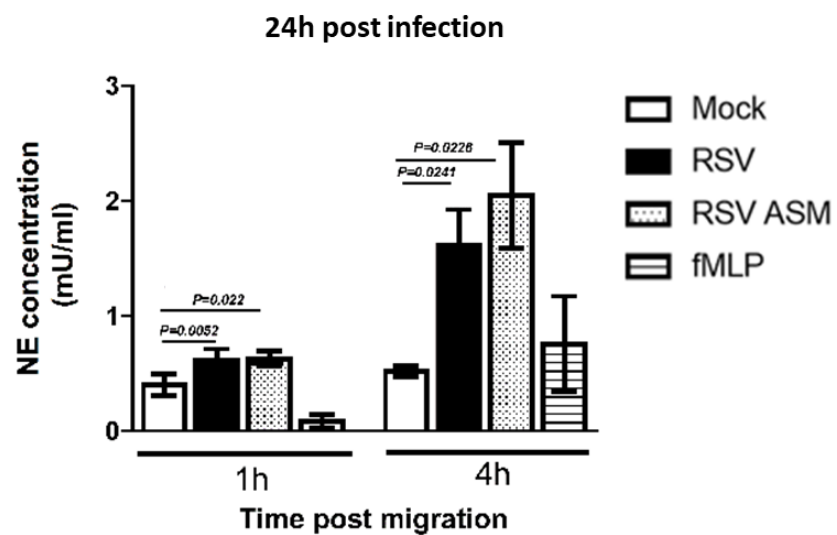
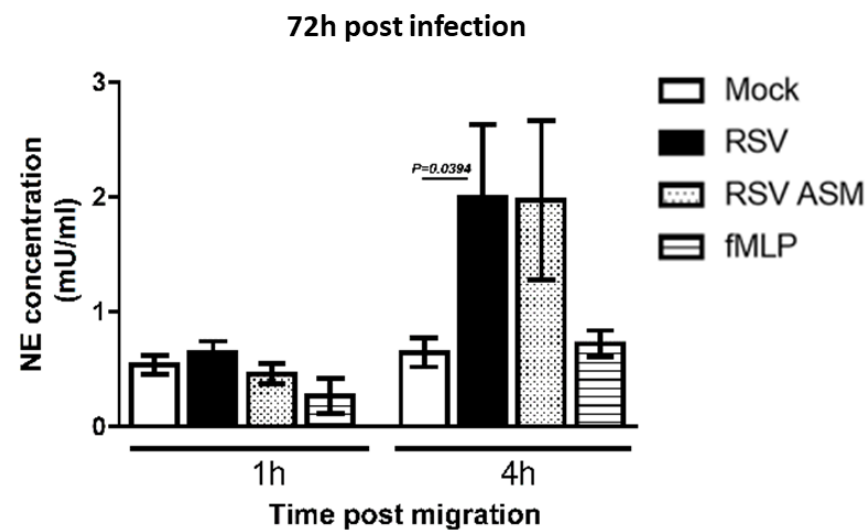
C**D**

Figure 5

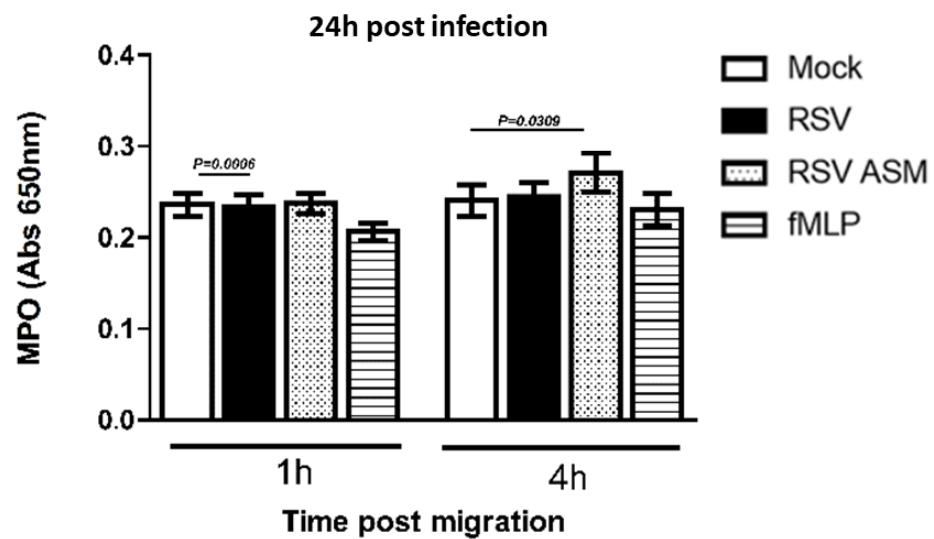
A



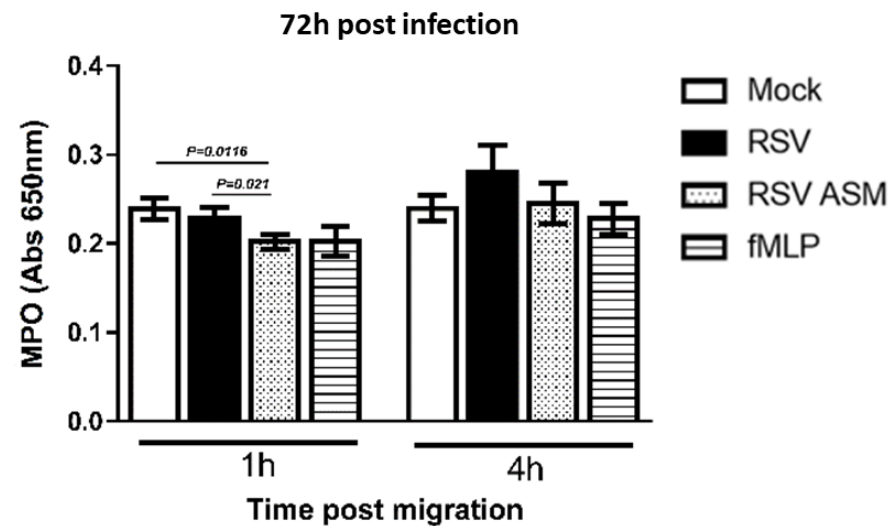
B

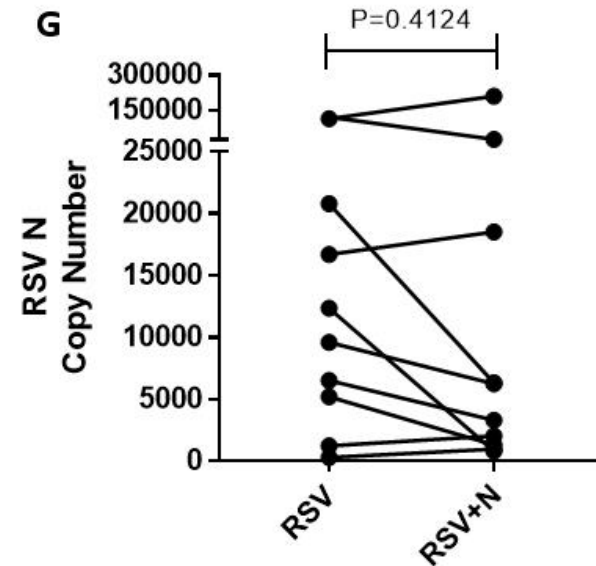
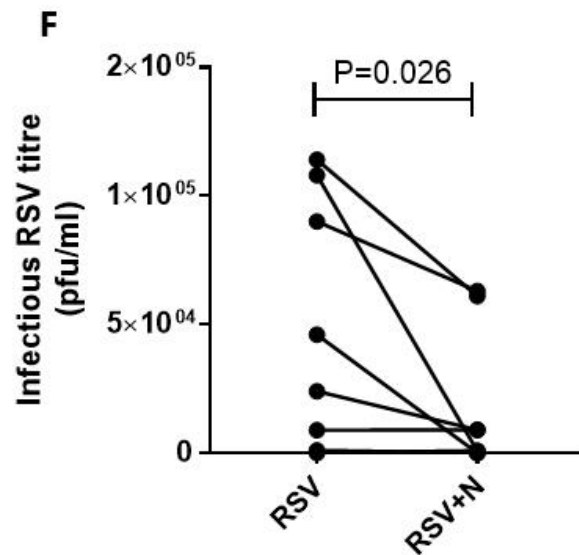
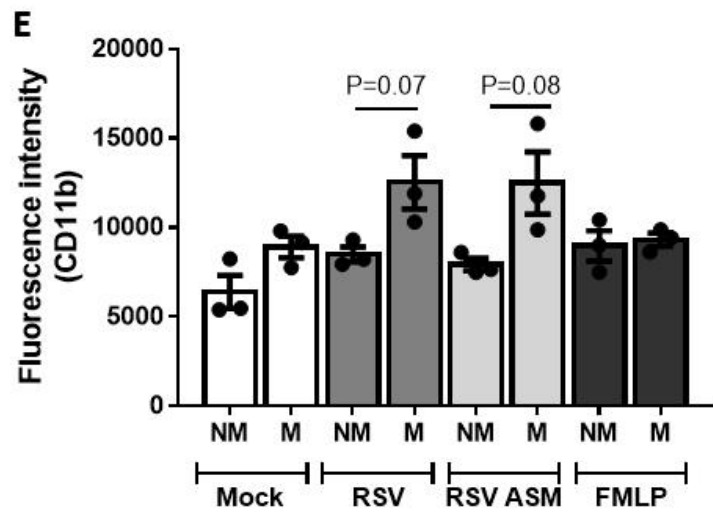


C

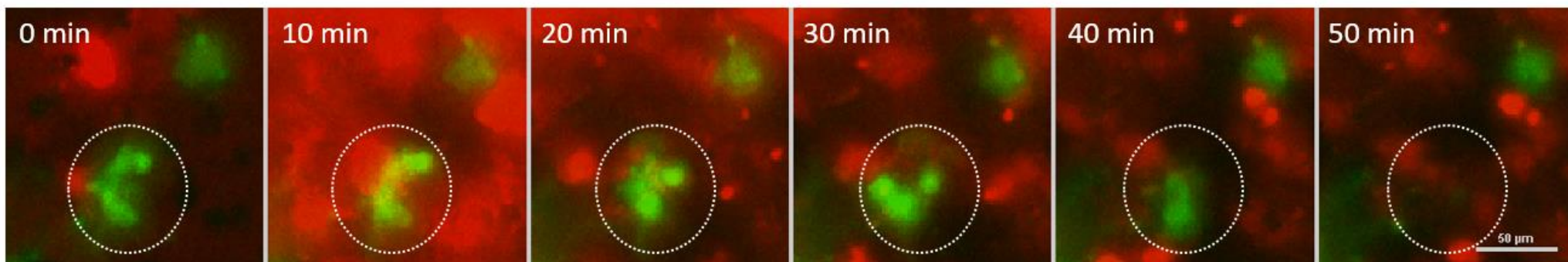


D





H



G

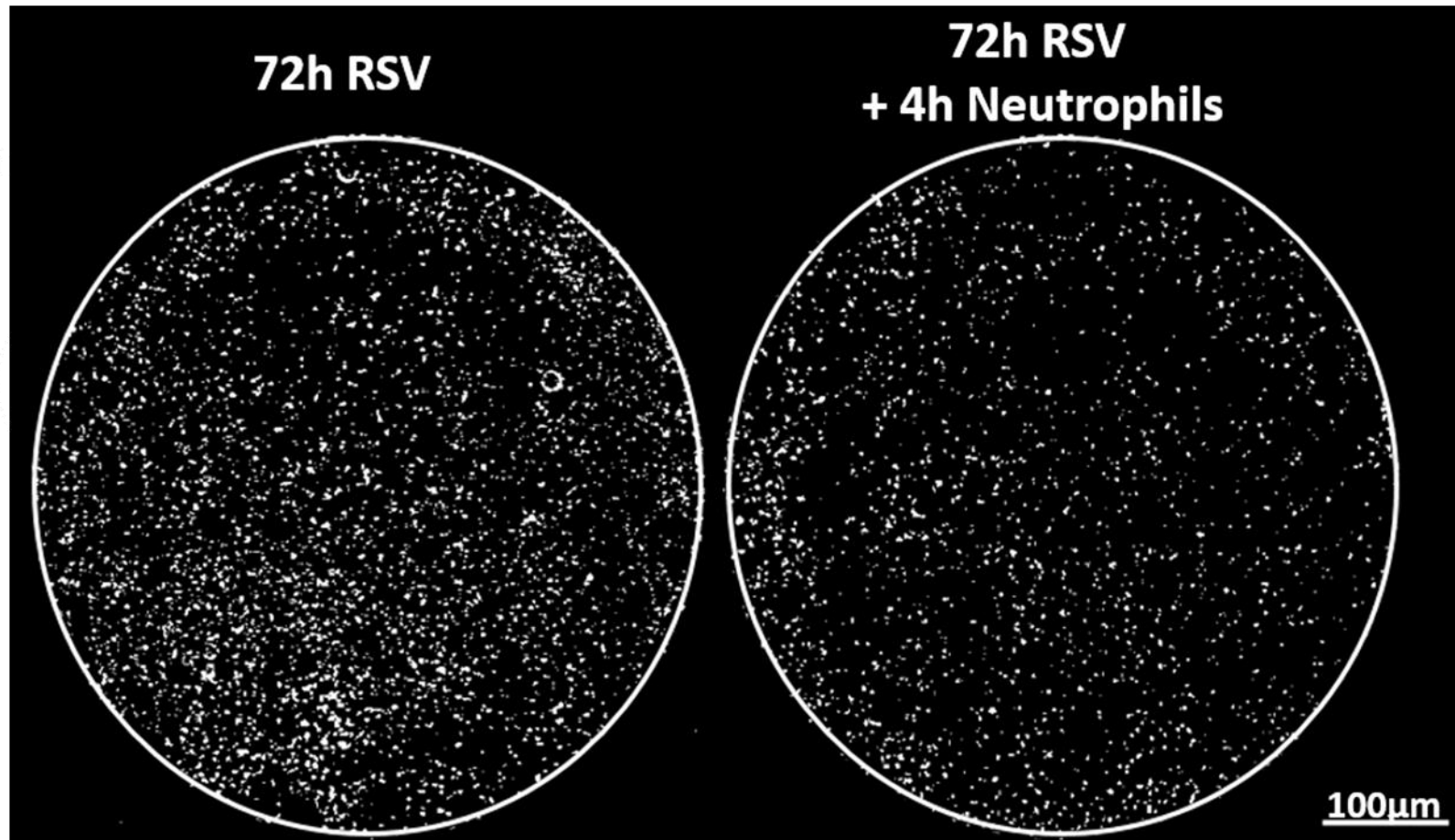
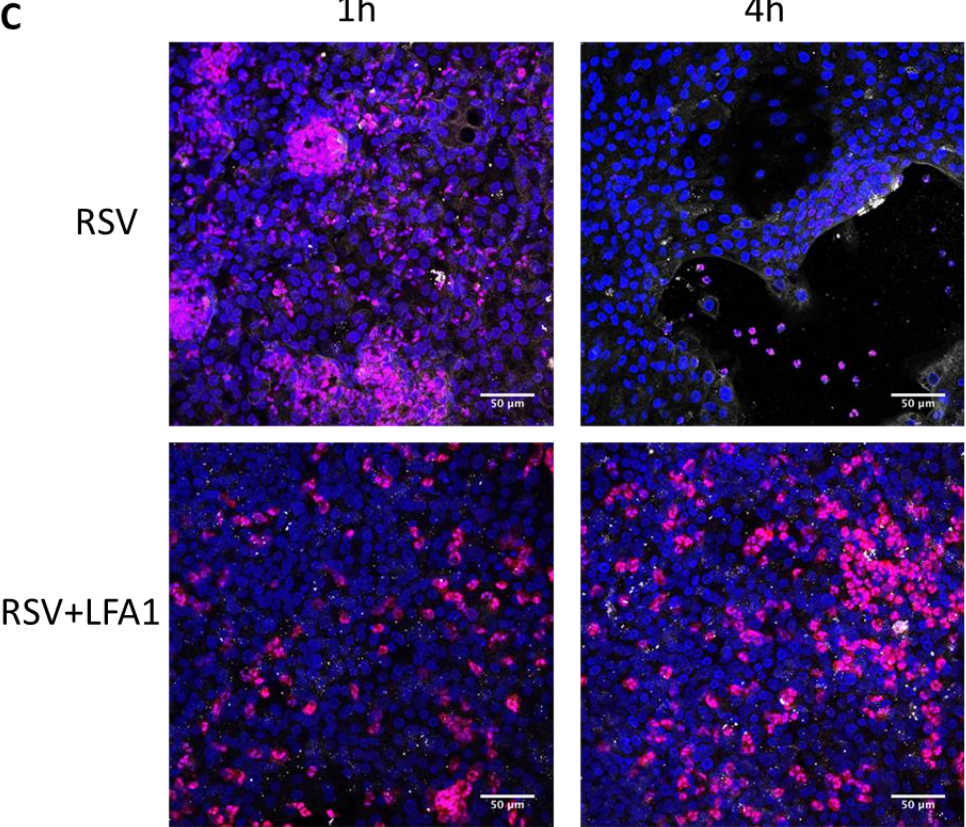
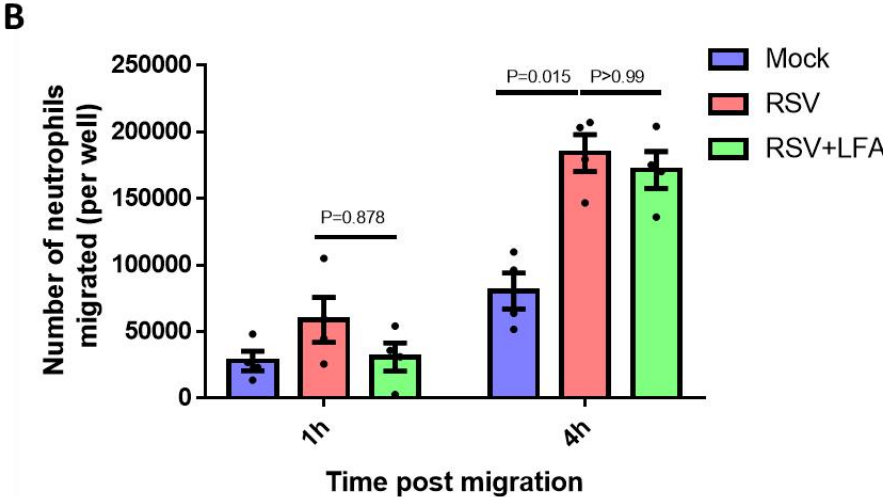
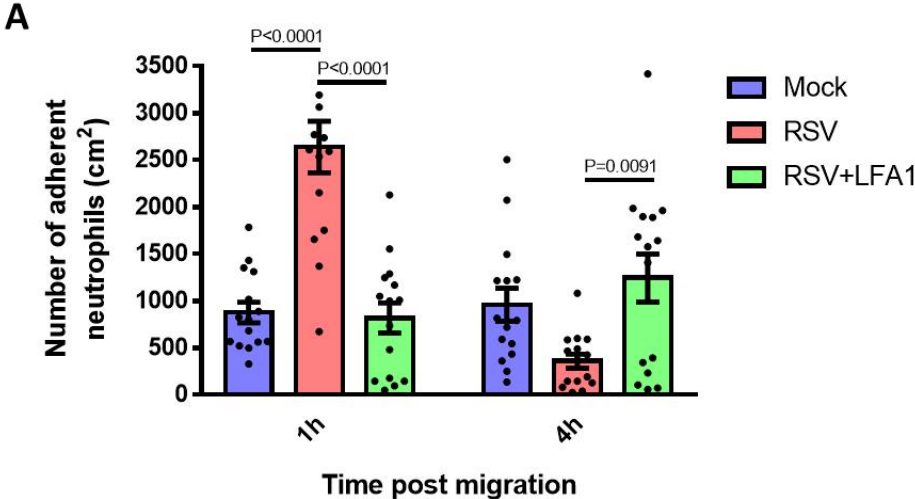
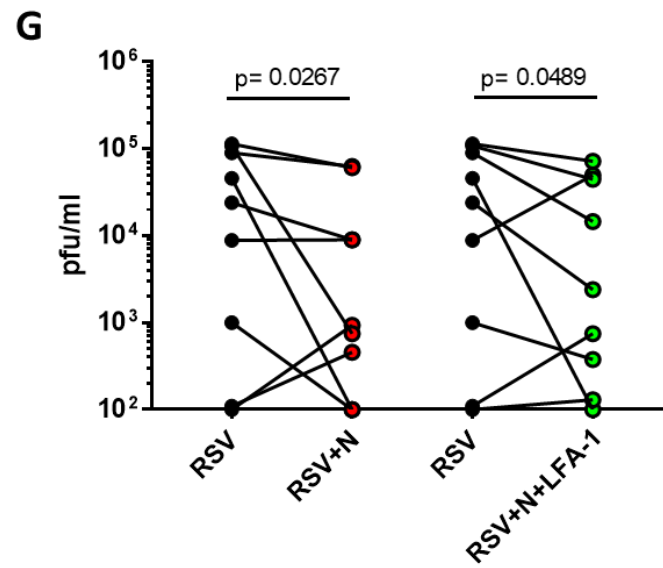
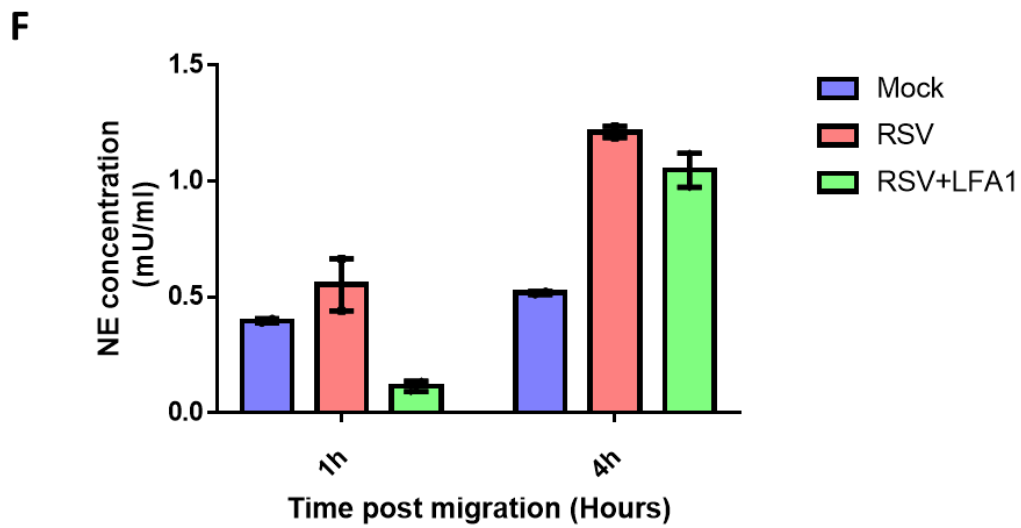
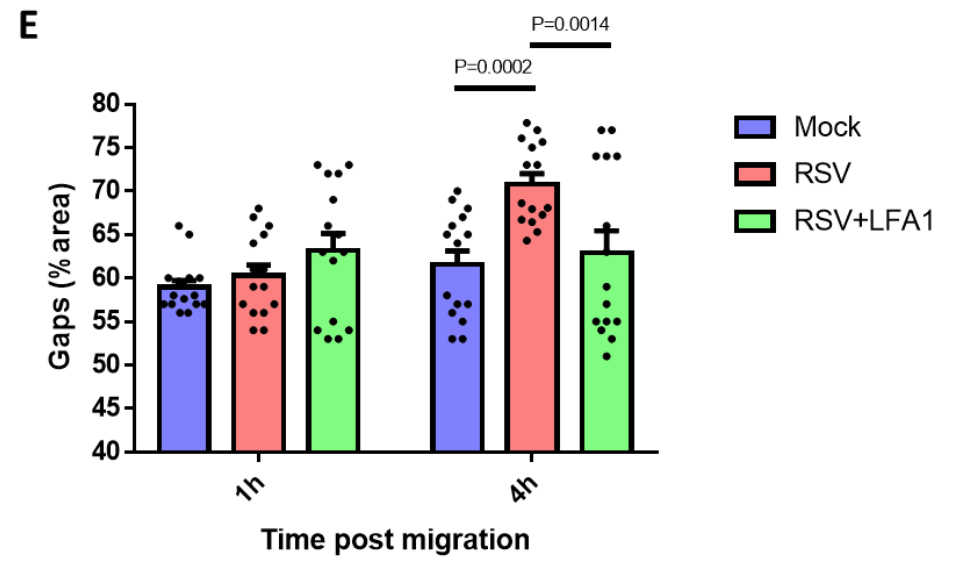
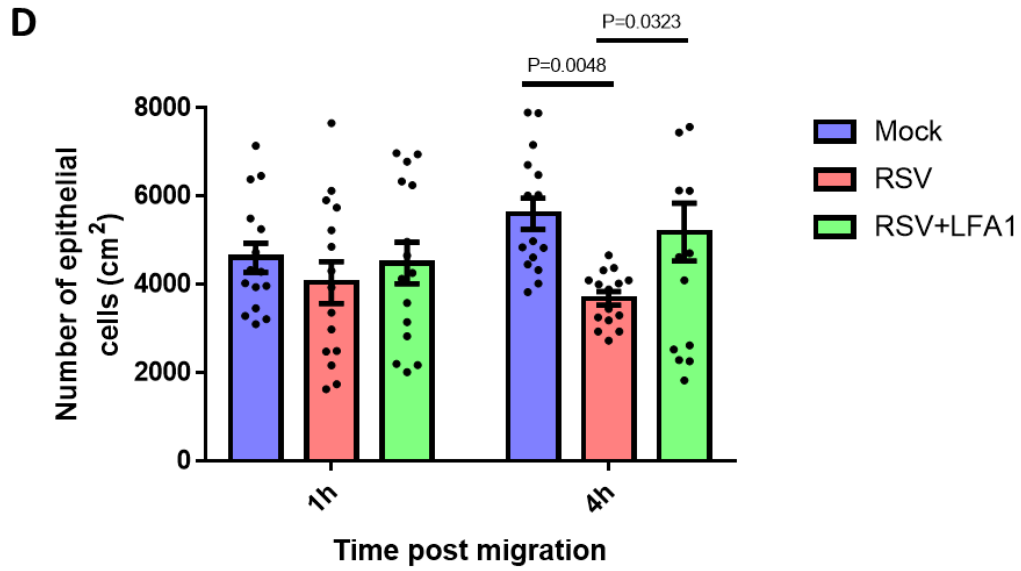


Figure 6





TITLE: β 2 integrin LFA1 mediates airway damage following neutrophil trans-epithelial migration during RSV infection. **METHODS**

AUTHORS AND AFFILIATIONS:

Jenny A. Herbert¹, Yu Deng^{1,2}, Elisabeth Robinson¹, Rosalind L. Smyth¹, Claire M. Smith¹
¹ Respiratory, Critical Care & Anaesthesia, Great Ormond Street Institute of Child Health, University College London (UCL), London, United Kingdom.

Corresponding author:

Claire Smith

c.m.smith@ucl.ac.uk

Tel: +44 (0)20 7905 2183

Email address of co-authors:

Jenny Herbert (Jenny.Herbert@ucl.ac.uk)

Yu Deng (y.deng@ucl.ac.uk)

Elisabeth Robinson (elisabeth.robinson.17@ucl.ac.uk)

Rosalind Smyth (rosalind.smyth@ucl.ac.uk)

A Video Methodology can be found here: <https://youtu.be/NRFRuriSWks>

PROTOCOL:

1. Isolation of primary AECs from nasal brushings

- 1.1. Collect airway epithelial cells by performing a nasal brushing on a healthy adult donor as described elsewhere¹⁴. Commercially available nasal epithelial cells (i.e. from Lonza or Epithelix Sarl) can also be used. The methods shown here can be used for cells obtained from both nasal brushings and commercially available human nasal epithelial cells.
- 1.2. Process nasal brushings cells immediately (i.e. go to step 1.3) or store in the fridge overnight in 2 ml M199 media supplemented with 2.5µg/ml amphotericin B, 100 U/ml penicillin and 100 µg/ml streptomycin.
- 1.3. Collect the nasal epithelial cells by centrifugation at 600xg.
- 1.4. Resuspend in F-media as is described elsewhere¹⁵ (F-media composition: Dulbecco's modified Eagle's medium (DMEM) and F12 at a 3:1 ratio with 100 U/ml penicillin and 100µg/ml streptomycin and 7.5% (v/v) fetal bovine serum supplemented with 5 mM Y-27632, hydrocortisone (25 ng/ml), epidermal growth factor (0.125 ng/ml), insulin (5 mg/ml), 0.1 nM cholera toxin, amphotericin B (2.50 µg/ml)).
- 1.5. Cells are ready to be seeded as described in section 2.2

2. Expansion of primary AECs using co-culture with 3T3-J2 feeder cell layers

All steps should be performed in a sterile environment using a Class II safety cabinet.

- 2.1. Prepare 3T3-J2 feeder layers as described previously¹⁵. Briefly:
 - 2.1.1. Culture 3T3-J2 mouse embryonic fibroblast in DMEM supplemented with 10% (v/v) calf serum, 100 U/ml penicillin and 100 µg/ml streptomycin until 70-80 % confluent.
 - 2.1.2. Add 150 µl of stock mitomycin (0.4 µg/ml in PBS) to a T175cm² flask of 3T3-J2 cells with 15 ml fresh media to mitotically inactivate cells.
 - 2.1.3. Incubate for 2 hours at 37°C 5 % CO₂.
 - 2.1.4. After incubation, remove all media by aspiration.
 - 2.1.5. Rinse 3T3-J2 cells with sterile PBS.
 - 2.1.6. Dissociate 3T3-J2 cells using 1x trypsin. Incubate flasks at 37°C 5 % CO₂ for roughly 5 minutes or until >95% cells are detached.
 - 2.1.7. Gently tap the T75cm² flasks to promote 3T3-J2 cellular detachment.
 - 2.1.8. Collect these cells in fresh PBS to inactivate trypsin and centrifuge at 200xg for 3 minutes.
 - 2.1.9. Resuspend the cell pellets in DMEM and count the number of viable cells using a haemocytometer and trypan blue exclusion.
 - 2.1.10. Seed cells at a density of 1x10⁶ / T75cm² flask in DMEM media and incubate at 37°C 5 % CO₂.
 - 2.1.11. 3T3-J2 feeder cells must be used within 48 hours of cell seeding. One confluent T175cm² flask of cells should make between 3-6 feeder flasks.
- 2.2. Seed primary AECs into feeder layers at a density of 5x10⁵/ flask. Seed cells directly into one or two 3T3-J2 feeder layers for propagation. A vial of commercial frozen AECs can

be split into two 3T3-J2 feeder flasks. AECs should not be used beyond passage 5 as they will not differentiate.

- 2.3. AECs are ready for use once the flasks are nearly confluent. To separate the 3T3-J2 fibroblasts from the basal cells expose them to differential concentrations of trypsin. 3T3-J2 are more sensitive to trypsin so should dissociate first while the AECs remain attached for a longer period. To do this:
 - 2.3.1. Aspirate media from T75cm² flasks and rinse cells in sterile PBS.
 - 2.3.2. Add 2ml of 1x Trypsin/ EDTA to each flask. Make up a 1x working trypsin solution by diluting the 10X stock in sterile PBS.
 - 2.3.3. Incubate flasks at 37°C 5 % CO₂ for roughly 5 minutes or until >95% fibroblasts are detached
 - 2.3.4. Gently tap the T75cm² flasks to promote 3T3-J2 cellular detachment, the AECs should remain attached.
 - 2.3.5. Rinse flasks in PBS to inactivate trypsin and remove residual fibroblasts.
 - 2.3.6. Detach and dissociate the remaining AECs. Add 2ml of trypsin and incubating for 5-10-minutes at 37°C 5 % CO₂.
 - 2.3.7. Collect these cells in fresh F-media and centrifuge at 200xg for 3 minutes.
 - 2.3.8. Resuspend the cell pellets in F-media and count the number of viable cells using a Neubauer haemocytometer and trypan blue exclusion.

3. Collagen coating permeable membrane inserts.

All steps should be performed in a sterile environment using a Class II safety cabinet.

- 3.1 Make collagen coating solution: dilute 3 mg/ml type I collagen stock 1:100 in sterile PBS (30 µg/ml working stock).
- 3.2 Remove a 24 well polyethylene terephthalate (PET) membrane insert with 3 µm pore size from sterile packaging and place in a new 24 well plate.
- 3.3 Coat membrane insert on both sides of the membrane.
 - 3.3.1 Add 100 µl of collagen working solution to the top of all membrane insert.
 - 3.3.2 Invert plate and remove plate bottom (membrane insert are now standing upright on the plate lid). The collagen solution below the membrane insert membrane remains in place by surface tensions. Ensure the solution does not drip down the side of the membrane insert.
 - 3.3.3 Add 100 µl of collagen working solution to the other side of the membrane insert.
 - 3.3.4 Replace the 24 wells plate to cover the membrane insert ensuring not to disturb the collagen solution.
 - 3.3.5 Incubate the membrane insert at room temperature for at least one hour.
- 3.4 After incubation aspirate collagen solution from both sides of the membrane insert membrane.
- 3.5 Rinse membrane insert with sterile water on both side of membrane and return to 24 well plate.
- 3.6 Leave lid off plate and allow membrane insert to dry in the tissue culture hood for 1 hour.

3.7 Replace lid and seal plates using parafilm. Store plates at room temperature for up to a month.

4. Seeding AECs onto permeable membrane inserts.

All steps should be performed in a sterile environment using a Class II safety cabinet.

- 4.1. Invert a collagen coated 24 well membrane insert in a sterile 12 well plate (one membrane insert/ well).
- 4.2. Seed AECs onto the bottom of the 3 μ m pore membrane insert membrane at a density of 300,000/cm² in 70 μ l of F-media. Place the lid over the plate and incubate at 37°C 5 % CO₂ for 4-6 hours. The 3 μ m membrane insert from Greiner have 0.6 x 10⁶/cm² pores, this is a lower density than the other commercially available from Greiner and the Corning (2 x 10⁶/cm²). We found that the higher pore density membrane inserts impair the ability to visualize cells on the membrane and to measure ciliary beat frequency.
- 4.3. After incubation invert the membrane inserts into a 24 well plate.
- 4.4. Aspirate any media on the membrane inserts.
- 4.5. Add 500 μ l of fresh F-media underneath the membrane inserts.
- 4.6. Add 100 μ l of F-media supplemented with 30 μ g/ml Collagen I and 5 % (v/v) Matrigel on the top of the membrane inserts.
- 4.7. Incubate cells for 24-48 hours at 37°C 5 % CO₂.
- 4.8. After this period, aspirate media from both sides of the membrane insert membrane and feed cells with 100 μ l of ALI media (ratio of 1:1 DMEM:Airway epithelial cell growth media) all supplements added, further supplemented with 2.5 μ g/ml amphotericin B, 100 U/ml penicillin, 100 μ g/ml streptomycin and 1 μ m retinoic acid. Make up fresh retinoic acid as a 100 mM stock in 100 % ethanol. Cells are now at air-liquid interface (ALI).
- 4.9. Feed cells basolaterally every 1-2 days with fresh media,
- 4.10. Incubate at 37°C 5 % CO₂ in a high humidity incubator for 28 days to allow cellular differentiation.
 - 4.10.1. Place trays of sterile water containing disinfectant to increase humidity and prevent bacterial/ fungal growth inside a tissue culture (TC) incubator.
- 4.11. Prepare a control membrane insert by seeding cells onto the top of a 0.4 μ m or 3 μ m pore insert membrane at a density of 150,000/ cm². Feed these cultures basolaterally with 350 μ l of ALI media every 1-2 days.
- 4.12. Wash off any AECs that detach from the membrane during culture by adding 400 μ l of ALI media apically. Aspirate this media and discard.
- 4.13. Primary AECs should be used after 4 weeks of ALI culture, when motile cilia are observed under an inverted microscope equipped with a S Plan Fluor ELWD 20x ADM objective with working distance of (8.2 – 6.9mm) and numerical aperture 0.45 (Nikon) and an ORCA Flash 4.0 digital camera (Hamamatsu). Our images were acquired at a resolution of 0.22 μ m/pixel.

5. Preparation of virus for epithelial cell infection

5.1. Viral stocks preparation and quantification of viral titre is performed as described

previously¹². Propagate rgRSV expressing GFP in HEp-2 cells as described previously⁴.

6. RSV infection of differentiated AECs

All steps should be performed in a sterile environment using a Class II safety cabinet.

- 6.1. Prior to infection, rinse the apical side of the cells with 400µl ALI media to remove any detached epithelial cells.
- 6.2. Measure trans-epithelial electrical resistance (TEER) using an epithelial voltohmmeter to confirm cell integrity. Only cultures that give reading of $>200\Omega/\text{cm}^2$ should be used.
- 6.3. Aspirate basolateral and apical media is from both sides of the membrane insert.
- 6.4. Remove membrane insert from the 24 well plate and place upside down in a fresh 12 well plate.
- 6.5. Dilute your virus stock in ALI media to give a multiplicity of infection (MOI) of 5 in 25 µl. To calculate the amount of virus required for infection based the calculation on their being roughly 1×10^5 AECs present on the membrane insert membrane (a large number of cells dissociate during incubation for 4 weeks).
- 6.6. Pipette 25 µl of virus preparation on to the cell-side of each membrane insert, being careful not to touch the AECs. Note: place 25 µl of ALI media only onto the mock infected membrane inserts.
- 6.7. Replace the plate lid (ensuring the liquid does not touch the lid) and incubate membrane inserts at 37°C 5 % CO₂ for 1 hour. After incubation, wash cells in PBS to remove any excess liquid on the top of membrane inserts.
- 6.8. Place the membrane inserts in a fresh 24 well plate and add 100 µl of ALI media to the basolateral side of the cells. The apical side of membrane insert remains at ALI. Incubate at 37°C, 5 % CO₂ for 24-72 hours to allow progression of viral infection.

7. Isolation of neutrophils from whole blood

- 7.1. Isolate neutrophils from the whole blood of healthy adult donors or different patient groups.
- 7.2. Collect whole blood in 9 ml K3 EDTA Vacuette tubes, 21G needle and vacutainer adaptor (other volume tubes can be used).
- 7.3. Remove 1ml of blood and place in 1.5ml microfuge tube. Leave at room temperature with lid open for 20 minutes to form a buffy coat. Carefully close lid and centrifuge at 2000xg for 10 minutes. Collect the top layer and place in new microfuge tube. Store on ice until needed.
- 7.4. Purify neutrophils using a direct human neutrophil isolation kit (STEMCELL), as per the manufacturer's instructions.
- 7.5. Resuspend neutrophils in HBSS- (calcium/ magnesium negative).
- 7.6. Neutrophils can be stained if required for the transmigration assay. To do this:
 - 7.6.1. Incubate roughly 1×10^7 neutrophils with 1 µl of stock dye (calcein red orange dye (6.25 µg/µl in DMSO))
 - 7.6.2. Incubate for 30 minutes at room temperature in the dark.
 - 7.6.3. Wash cells in HBSS- and resuspend in HBSS+ (calcium/ magnesium positive).
- 7.7. Count cells with a Neubauer haemocytometer. Neutrophils are then ready to be added

to the basolateral side of the membrane insert for migration.

8. Preparation of differentiated AECs for neutrophil migration assay

All steps should be performed in a sterile environment using a Class II safety cabinet.

- 8.1. On the morning of the neutrophil migration assay, place 600 μ l of ALI media under the membrane insert for 30 minutes to allow collection of chemokines/ cytokines produced from RSV/ mock infected AECs.
- 8.2. Collect and pool the original apical supernatant from each test condition. Groups used in the assay include Mock, RSV infected controls.
 - 8.2.1. Centrifuge at 1000xg for 3 minutes and discard the pellet containing any detached epithelial cells.
- 8.3. Place the membrane inserts into new ultra-low binding 24 well plates. Neutrophils do not adhere to the surface of these plates so can be collected post-transmigration.
- 8.4. Replace 400 μ l of the supernatant underneath the corresponding test condition. Aliquot and store any remaining supernatant at -20°C for future analysis.
- 8.5. For a positive control, add 400 μ l of 100nm fMLP (4 mg/ml stock in DMSO) in HBSS+ to the underside of a mock infected membrane insert.
- 8.6. Collect basolateral supernatants from each insert, aliquot and store at -20°C for future studies.
- 8.7. Return the plate to the incubator until the neutrophils are ready.

9. Neutrophil transmigration assay

All steps should be performed in a sterile environment using a Class II safety cabinet

- 10.1. Add 5×10^5 neutrophils in HBSS+ containing 1 % (v/v) autologous serum (collected from the whole blood see 8.3) to the basolateral side of each membrane insert.
- 10.2. Incubate plates at 37°C , 5 % CO_2 for 1-4 hours. Different time points can be used depending on the experiment.
- 10.3. After migration, collect neutrophils from the apical side of the epithelial cells (these are now referred to as the migrated neutrophils) and basolateral side (the non-migrated neutrophils) in a microfuge tube.
- 10.4. If the neutrophils were pre-stained, quantify the number migrated using a plate reader and compare to a standard curve of known numbers of stained neutrophils, as described previously¹².
- 10.5. Collect supernatants from the basolateral and apical side of the membrane insert; aliquot and store at -20°C for future analysis.
- 10.6. Fix membrane insert in 1 % (v/v) PFA and stain for neutrophil or epithelial cell markers of interest.

10 Analysis of ciliary function during neutrophil transmigration

- 10.1 To measure ciliary beat frequency, place membrane inserts a 24 well plate in an incubation chamber at 37°C and 5% CO_2 attached to an inverted microscope system.
- 10.2 Equilibrate cells for at least 30 minutes before image capture.
- 10.3 Record beating cilia using a digital video camera at a rate of 200 frames per

second and capture at least 512 frames. The video area (512 x 512 pixels) should contain at least 10 ciliated cells. For each condition, at least 5 areas of the membrane insert should be videoed for CBF analysis.

10.4 Save files as an .AVI and calculate CBF by fast Fourier transformation using open-sourced ciliaFA software as previously described¹⁶.

REFERENCES:

1. Smith, C. M. *et al.* Ciliary dyskinesia is an early feature of respiratory syncytial virus infection. *Eur Respir J* **43**, 485–496 (2014).
2. McNamara, P. S., Ritson, P., Selby, A., Hart, C. A. & Smyth, R. L. Bronchoalveolar lavage cellularity in infants with severe respiratory syncytial virus bronchiolitis. *Arch Dis Child* **88**, 922–926 (2003).
3. Sacco, R. E., Durbin, R. K. & Durbin, J. E. Animal models of respiratory syncytial virus infection and disease. *Curr Opin Virol* **13**, 117–122 (2015).
4. Zhang, L., Peeples, M. E., Boucher, R. C., Collins, P. L. & Pickles, R. J. Respiratory syncytial virus infection of human airway epithelial cells is polarized, specific to ciliated cells, and without obvious cytopathology. *J Virol* **76**, 5654–5666 (2002).
5. Villenave, R. *et al.* In vitro modeling of respiratory syncytial virus infection of pediatric bronchial epithelium, the primary target of infection in vivo. *Proc Natl Acad Sci U S A* **109**, 5040–5045 (2012).
6. Tristram, D. A., Hicks, W. & Hard, R. Respiratory syncytial virus and human bronchial epithelium. *Arch Otolaryngol Head Neck Surg* **124**, 777–783 (1998).
7. Villenave, R. *et al.* Differential cytopathogenesis of respiratory syncytial virus prototypic and clinical isolates in primary pediatric bronchial epithelial cells. *Virol J* **8**, 43 (2011).
8. Persson, B. D., Jaffe, A. B., Fearn, R. & Danahay, H. Respiratory syncytial virus can infect basal cells and alter human airway epithelial differentiation. *PLoS ONE* **9**, e102368 (2014).
9. Weppler, A. & Issekutz, A. C. Alveolar epithelium down-modulates endotoxin-but not tumor necrosis factor alpha-induced activation of endothelium and selectively inhibits neutrophil transendothelial migration. *Exp Lung Res* **34**, 425–453 (2008).
10. Weppler, A., Rowter, D., Hermanns, I., Kirkpatrick, C. J. & Issekutz, A. C. Modulation of endotoxin-induced neutrophil transendothelial migration by alveolar epithelium in a defined bilayer model. *Exp Lung Res* **32**, 455–482 (2006).
11. Hurley, B. P., Williams, N. L. & McCormick, B. A. Involvement of phospholipase A2 in *Pseudomonas aeruginosa*-mediated PMN transepithelial migration. *Am J Physiol Lung Cell Mol Physiol* **290**, L703–L709 (2006).
12. Deng, Y., Herbert, J. A., Smith, C. M. & Smyth, R. L. An in vitro transepithelial migration assay to evaluate the role of neutrophils in Respiratory Syncytial Virus (RSV) induced epithelial damage. *Sci Rep* **8**, 6777 (2018).

13. Yonker, L. M. *et al.* Development of a Primary Human Co-Culture Model of Inflamed Airway Mucosa. *Sci Rep* **7**, 8182 (2017).
14. Chilvers, M. A. & O'Callaghan, C. Analysis of ciliary beat pattern and beat frequency using digital high speed imaging: comparison with the photomultiplier and photodiode methods. *Thorax* **55**, 314–317 (2000).
15. Butler, C. R. *et al.* Rapid expansion of human epithelial stem cells suitable for airway tissue engineering. *Am J Respir Crit Care Med* **194**, 156–168 (2016).
16. Smith, C. M. *et al.* ciliaFA: a research tool for automated, high-throughput measurement of ciliary beat frequency using freely available software. *Cilia* **1**, 14 (2012).
17. Hoonhorst, S. J. M. *et al.* Increased activation of blood neutrophils after cigarette smoking in young individuals susceptible to COPD. *Respir Res* **15**, 121 (2014).
18. Brockbank, S., Downey, D., Elborn, J. S. & Ennis, M. Effect of cystic fibrosis exacerbations on neutrophil function. *Int Immunopharmacol* **5**, 601–608 (2005).

Appendix

Key statistical tests used (Mock v RSV) using GraphPad Prism

Figure	Array 1	Array 2	N	Test used	P value	95% Confidence interval
2A	Mock 1h	RSV 1h	6	One tailed paired T Test	0.0356	-2782 to 47120
2A	Mock 4h	RSV 4h	6	One tailed paired T Test	0.0507	-
2B	Mock 1h	RSV 1h	6	One tailed paired T Test	0.0034	-3332 to 69622
2B	Mock 4h	RSV 4h	6	One tailed paired T Test	0.0009	51869 to 129873
2C	Mock 1h	RSV 1h	15	One tailed paired T Test	<0.0001	-1374 to -704.2
2C	Mock 4h	RSV 4h	15	One tailed paired T Test	0.0011	194.6 to 712.8
2D	Mock 1h	RSV 1h	15	One tailed paired T Test	<0.0001	-2328 to -1198
2D	Mock 4h	RSV 4h	15	One tailed paired T Test	0.0052	164.7 to 1037
3B	Mock 1h	RSV 1h	15	One tailed paired T Test	0.1418	-
3B	Mock 4h	RSV 4h	15	One tailed paired T Test	<0.0001	-13.19 to -5.252
3C	Mock 1h	RSV 1h	15	One tailed paired T Test	0.0507	-126.2 to 1256
3C	Mock 4h	RSV 4h	15	One tailed paired T Test	<0.0001	1102 to 2741
3D	Mock 1h	RSV 1h	4	One tailed paired T Test	0.4575	-
3D	Mock 4h	RSV 4h	4	One tailed paired T Test	0.0177	-0.3163 to -0.02174
4A	Mock 1h	RSV 1h	4	One tailed paired T Test	0.0052	-0.324 to -0.09367
4A	Mock 4h	RSV 4h	4	One tailed paired T Test	0.0241	-2.187 to -0.01673
4B	Mock 1h	RSV 1h	4	One tailed paired T Test	0.1654	-
4B	Mock 4h	RSV 4h	4	One tailed paired T Test	0.0394	-2.986 to 0.2875
4C	Mock 1h	RSV 1h	4	One tailed paired T Test	0.0006	-0.00315 to -0.00185
4C	Mock 4h	RSV 4h	4	One tailed paired T Test	0.4035	-
4D	Mock 1h	RSV 1h	4	One tailed paired T Test	0.0776	-
4D	Mock 4h	RSV 4h	4	One tailed paired T Test	0.0610	-
4E	RSV NM	RSV M	3	One tailed paired T Test	0.071	-
4E	ASM NM	ASM M	3	One tailed paired T Test	0.078	-
4F	RSV	RSV+N	9	One tailed paired T Test	0.0263	-55458 to 400.7
4G	RSV	RSV+N	10	One tailed paired T Test	0.4124	-

Key statistical tests used (RSV + RSV LFA1) using GraphPad Prism

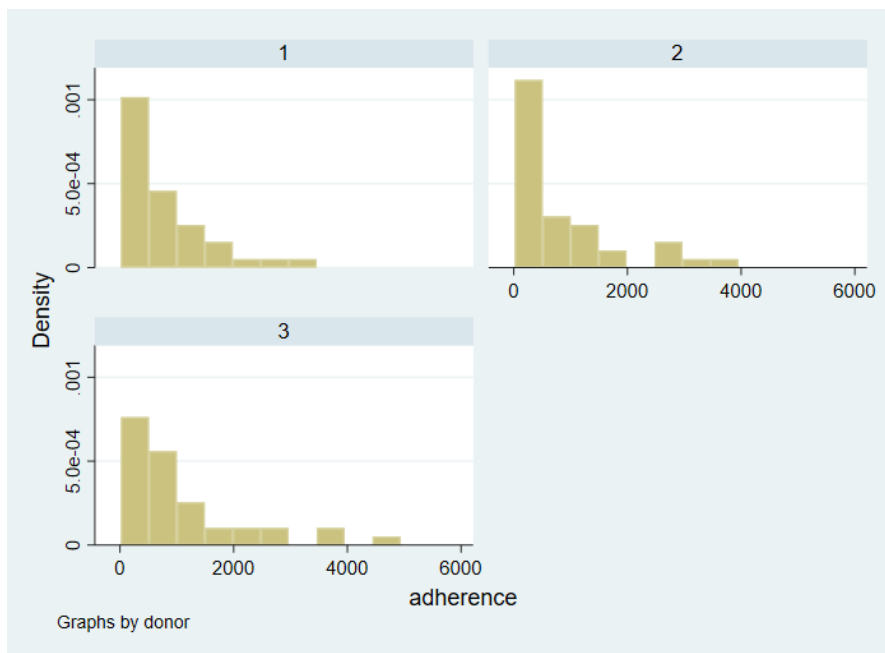
Figure	Array 1	Array 2	N	Test used	P value	95% Confidence interval
5A	Mock 1h	RSV 1h	15	Two way ANOVA with Bonferroni correction	<0.0001	-2458 to -1068
5A	RSV 1h	RSV+LFA 1h	15		<0.0001	1125 to 2515
5A	Mock 4h	RSV 4h	15	Two way ANOVA with Bonferroni correction	0.1081	-
5A	RSV 4h	RSV+LFA 4h	15		0.0091	-1581 to -191.4
5B	RSV 1h	RSV+LFA 1h	4	Two way ANOVA with Bonferroni correction	0.878	-
5B	RSV 4h	RSV+LFA 4h	4		>0.99	-
5D	Mock 4h	RSV 4h	15	Two way ANOVA with Bonferroni correction	0.0048	521.7 to 3322
5D	RSV 4h	RSV+LFA 4h	15		0.0323	-2902 to -101.9
5E	Mock 4h	RSV 4h	15	Two way ANOVA with Bonferroni correction	0.0002	-14.34 to -4.232
5E	RSV 4h	RSV+LFA 4h	15		0.0014	2.832 to 12.94
5G	RSN+N	RSV+N+LFA	9	Wilcoxon matched-pairs signed rank test	0.9102	-

Statistical modelling using STATA

To validate our statistical tests were appropriate we carried out further analysis of the neutrophil adherence data using STATA. The results of this analysis are shown below:

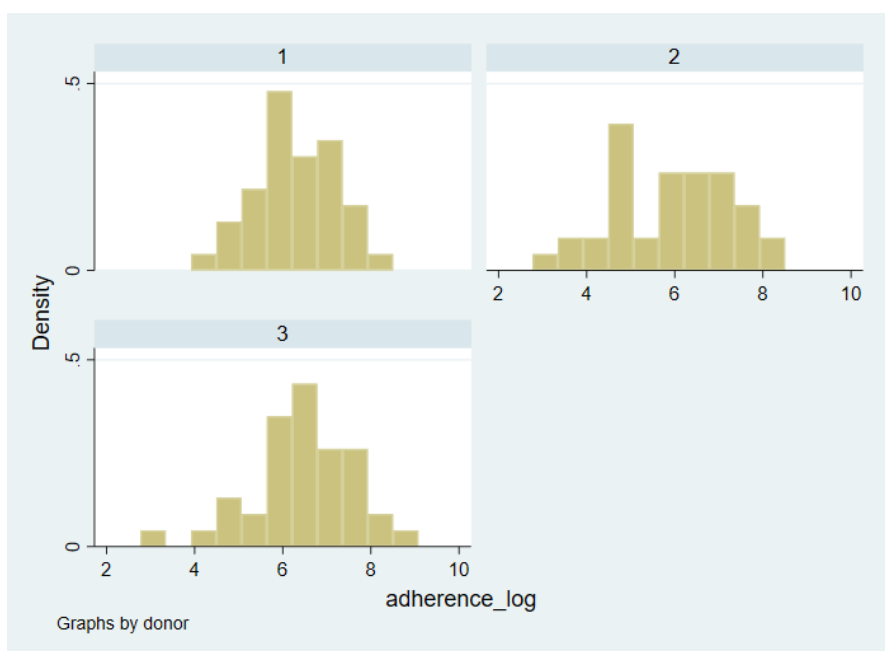
Linear mixed models, allowing for clustering by donor, ratio scale

Histogram Adherence at 1 hour - ratio scale (not normally distributed)



Linear mixed models, allowing for clustering by donor, log scale

Histogram Adherence at 1 hour - log scale (normally distributed)



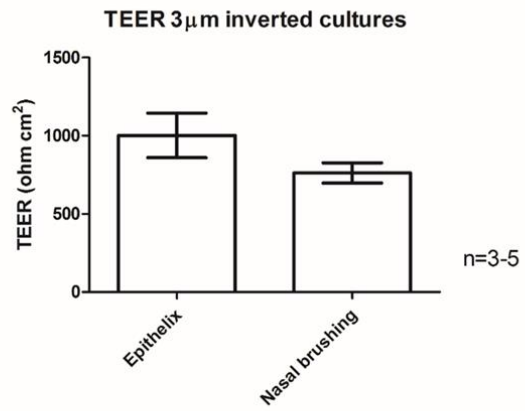
T test of normally distributed data

<i>adherence_~g</i>	<i>Coef.</i>	<i>Std. Err.</i>	<i>z</i>	<i>P>z</i>	<i>[95% Conf.]</i>	<i>Interval]</i>
<i>type_n</i>						
<i>M_R</i>	0.190656	0.278341	0.68	0.493	-0.35488	0.736193
<i>RSV</i>	1.114467	0.278341	4.00	0.000	0.56893	1.660005
<i>fMLP</i>	-1.07402	0.278341	-3.86	0.000	-1.61955	-0.52848
<i>_cons</i>	6.669411	0.19814	33.66	0.000	6.281063	7.057759
<i>sigma_u</i>	0.039606					
<i>sigma_e</i>	0.762267					
<i>rho</i>	0.002692	(fraction of variance due to u_i)				

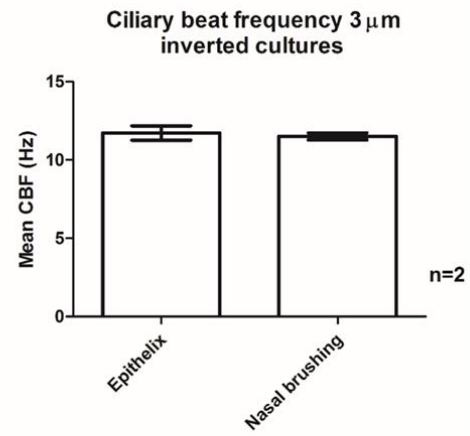
Supplementary Figures

Figure S1 – Quality control of primary differentiated airway epithelial cells cultures grown from commercially source (Epithelix) or from a nasal brushing on 3 μm pore membrane inserts. A- Trans-epithelial electrical resistance (TEER) was measured on cultures at day 28 post-ALI. B- Ciliary beat frequency (Hz) of beating cilia as measured after 28 days post-ALI. C - Airway epithelial cells stained by immunofluorescence with a marker of epithelial tight junctions (ZO-1; green), cilia (beta tubulin; red), and 49,6-diamidino-2-phenylindole (DAPI; blue) after 28 days of culture (scale bar, 50 μm).

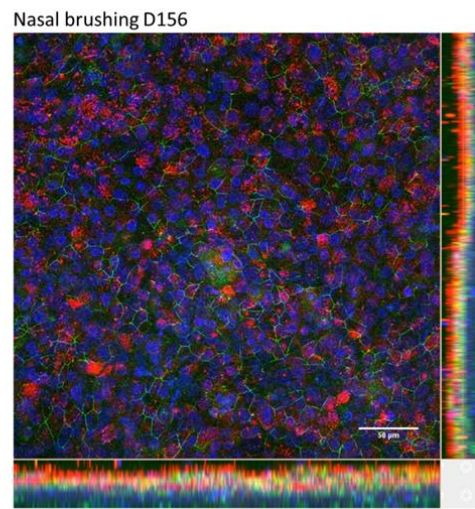
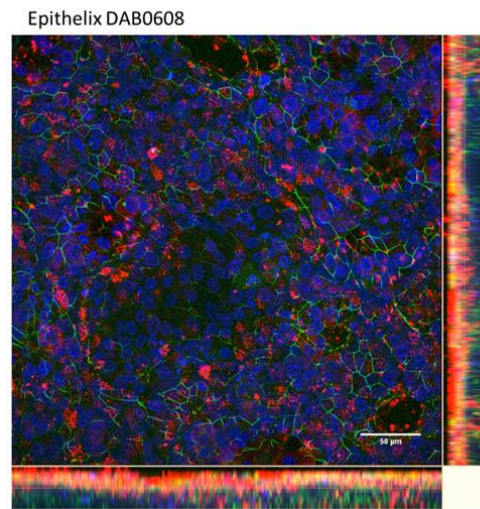
A



B



C



Red - Cilia
(beta tubulin)
Green - ZO-1
Blue - DAPI

D

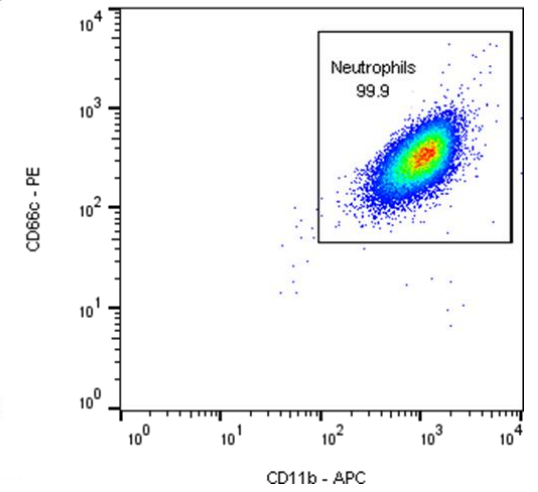
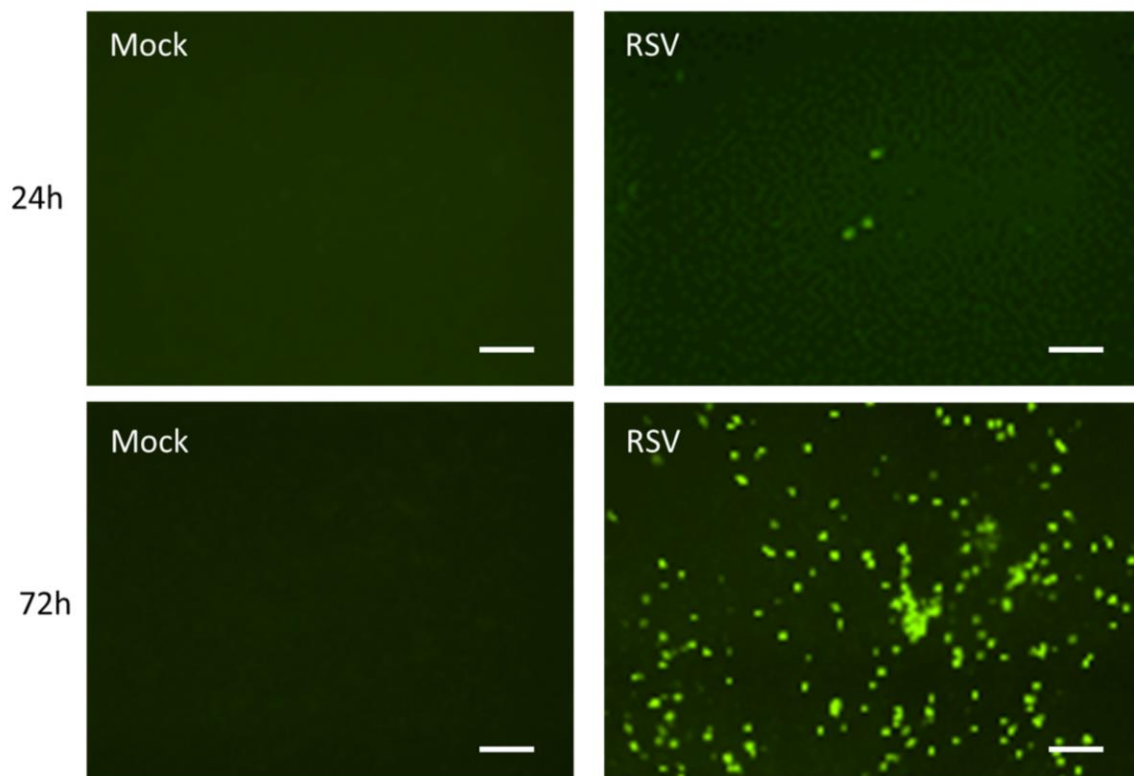


Figure S2- Viral replication, damage and inflammatory response of ciliated epithelial cells during RSV infection. A - Airway epithelial cells infected with mock (left panels) or RSV-GFP (right panels) after 28 days of culture on 3 μm pore membrane. Cells were visualized on fluorescence microscope 24h (top panels) or 72h (bottom panels) post infection. The recombinant RSV we used expresses GFP when replicating in AECs and therefore infected cells can be visualized without fixation and antibody staining (scale bar, 50 μm). **(B)** Lactate dehydrogenase (LDH) release from apical supernatant of cultures infected with mock control or RSV for 24h or 72h. **(C)** TEER was measured using a voltohmmeter, **(D)** Passive movement from basolateral to apical compartments was quantified using red-dextran leakage. **(E)** IL-8 **(F)** CXCL10 **(G)** Western blot of proteins associated with tight junction formation. Statistical comparison between all groups was performed using a paired t-test. For all bars show mean \pm SEM of $n = 3-5$ biological repeats unless otherwise stated. Statistical significance is shown. **(H)** ICAM1 expression on ciliated epithelial cells when infected with mock control or RSV for 24h or 72h as measured by fluorescence intensity. The mean (\pm SEM) fluorescence intensity from all images is shown (5 images per donor, 3 donors). We found that no significant difference in ICAM-1 expression at 24h post RSV infection compared to the Mock group. However, after 72h RSV infection there was significant increase in ICAM1 expression compared to the mock infected AECs. **(I)** Representative microscopy images of ciliated epithelial monolayers RSV infected for 24 and 72 hours, stained with ICAM1 (red) and nuclei stain (blue) are shown. Statistical comparison between all groups was performed using a paired t-test. For all bars show mean \pm SEM of $n = 3-4$ biological repeats unless otherwise stated. Statistical significance is shown.

A



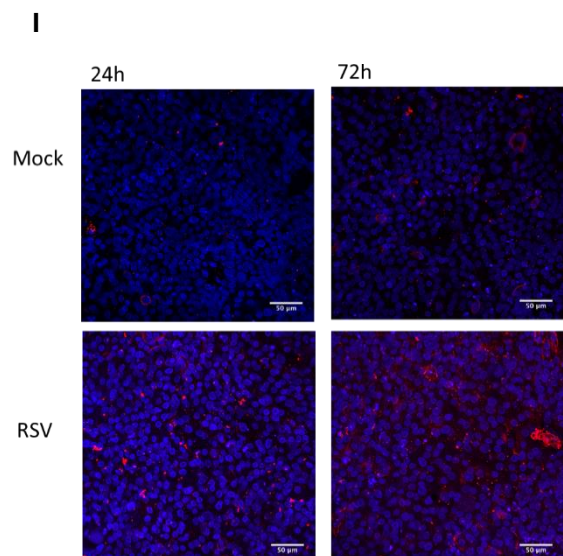
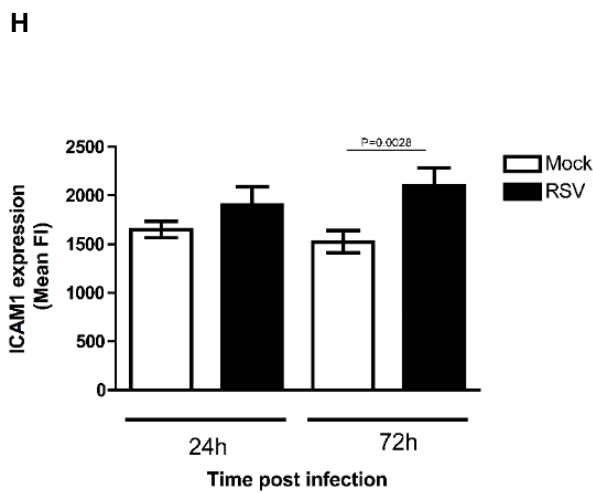
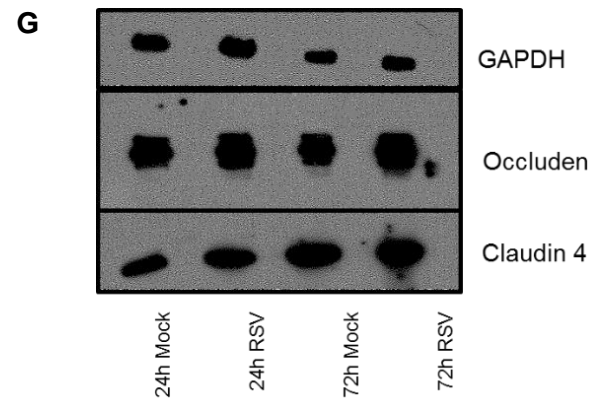
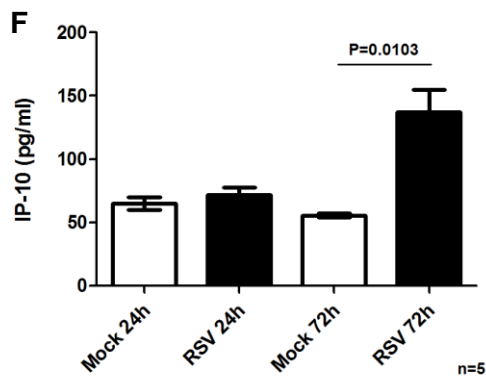
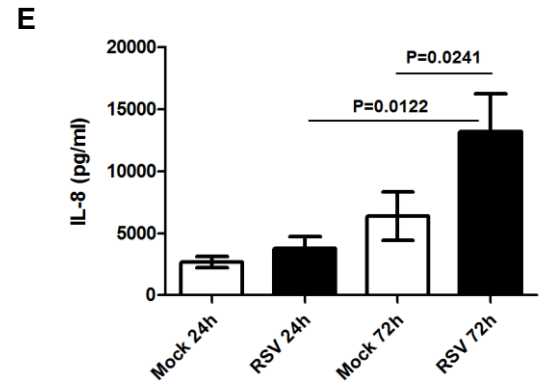
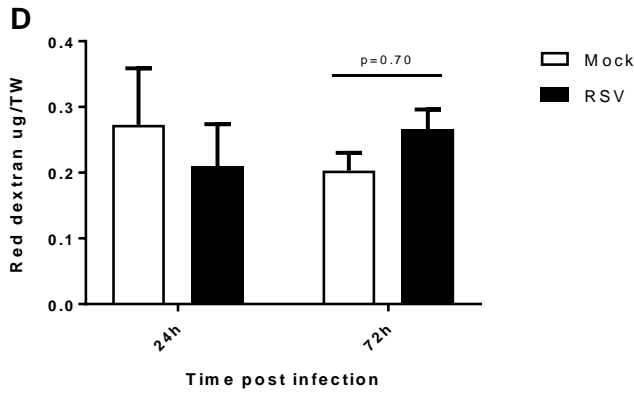
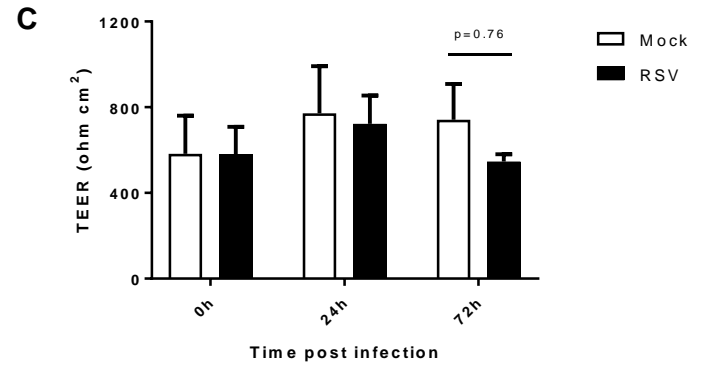
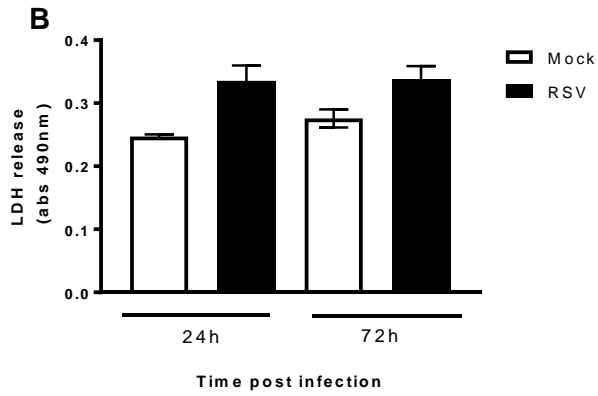


Figure S3. Damage caused by neutrophil trans-epithelial migration through ciliated epithelium infected with RSV for 24h (A) Gap analysis of areas with no epithelial DAPI staining (B) The number of epithelial cells attached to membrane inserts after 24h (F) or 72h (G) infection and 1 and 4 hours after neutrophil migration. Epithelial cells were quantified by counting the DAPI stained nuclei $>50\mu\text{m}^2$ in area using ImageJ. (C) Trans-epithelial electrical resistance (TEER) of each well as measured using a voltohmmeter. (D) Lactate dehydrogenase (LDH) release was measured in apical surface media of nAECs post neutrophil migration. Bars represent the mean \pm SEM for cultures mock infected (white bars), RSV infected (black bars), mock infected and exposed to RSV apical surface media (checkered bars) or mock infected and exposed apically to the chemoattractant fMLP (striped bars). Statistical comparison between all groups was performed using a paired t-test. For all bars show mean \pm SEM (n=4 epithelial donors, 3 heterologous and 1 homologous blood donors). * represents a significant different between the matched 1h and 4h migration time points.

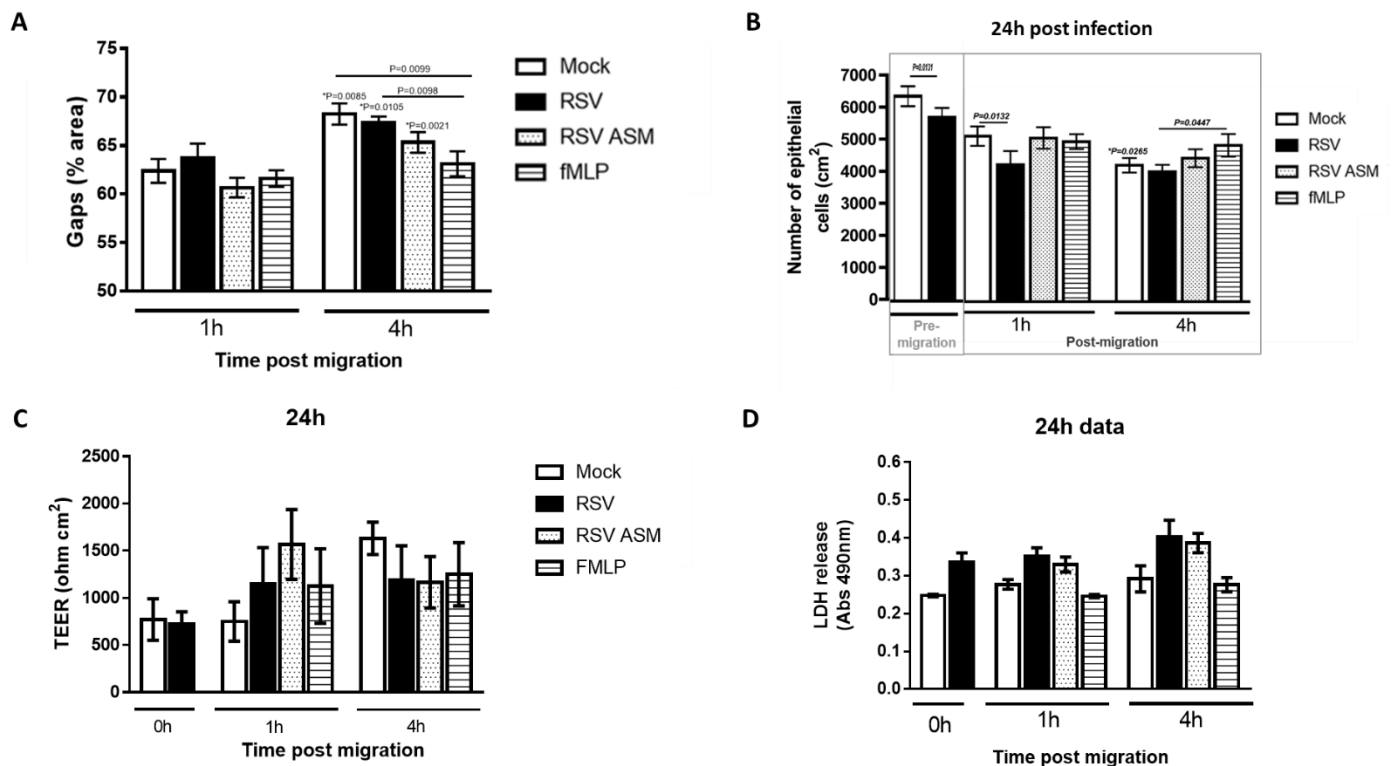


Figure S4 Damage caused by neutrophil trans-epithelial migration through RSV infected ciliated epithelium (A/B) Red-dextran (ug/well) flux from basal to apical compartments was quantified after 1 and 4 hours post neutrophil migration. Bars represent the mean \pm SEM for cultures mock infected (white bars), RSV infected (black bars), mock infected and exposed to RSV apical surface media (checkered bars) or mock infected and exposed apically to the chemoattractant fMLP (striped bars). Statistical comparison between all groups was performed using a paired t-test. For all bars show mean \pm SEM of n = 3-4 biological repeats unless otherwise stated. Statistical significance is shown.

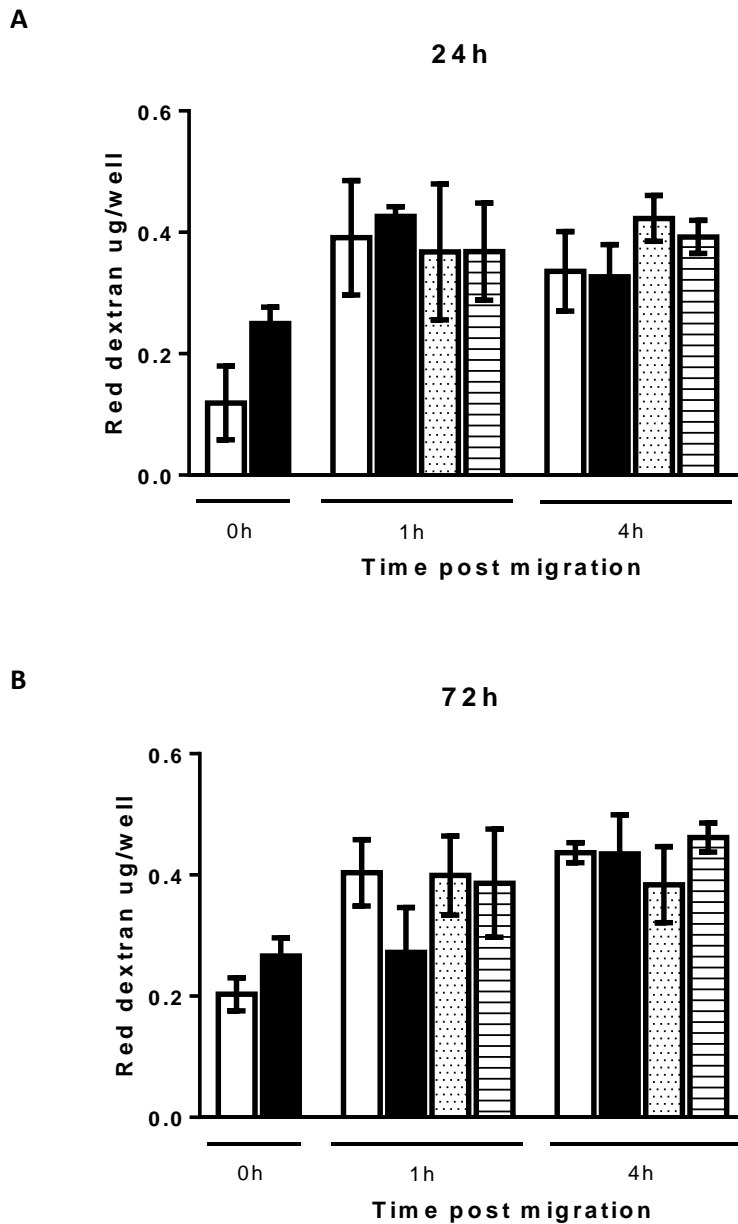


Figure S5 The accumulation of human neutrophils on the basolateral side of respiratory syncytial virus (RSV)-infected human nasal ciliated epithelial cells grown at an air–liquid interface. Images show the same area captured by live-confocal imaging of a 10um Z-stack (4 steps x 2.5um interval) on the basolateral side (top) of the 3um membrane insert following the addition of 5×10^5 calcein red-orange stained neutrophils (red) for up to 4 hours. Scale bar represents 100um.

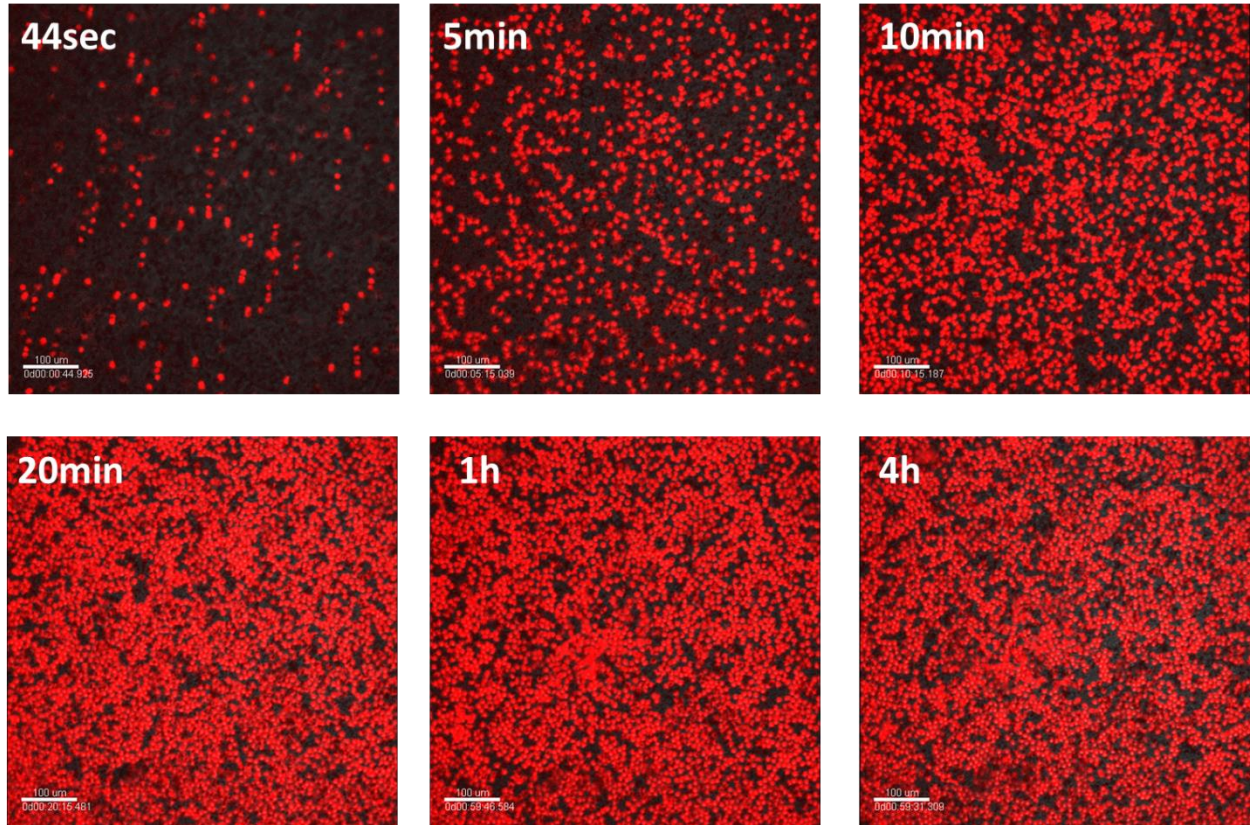
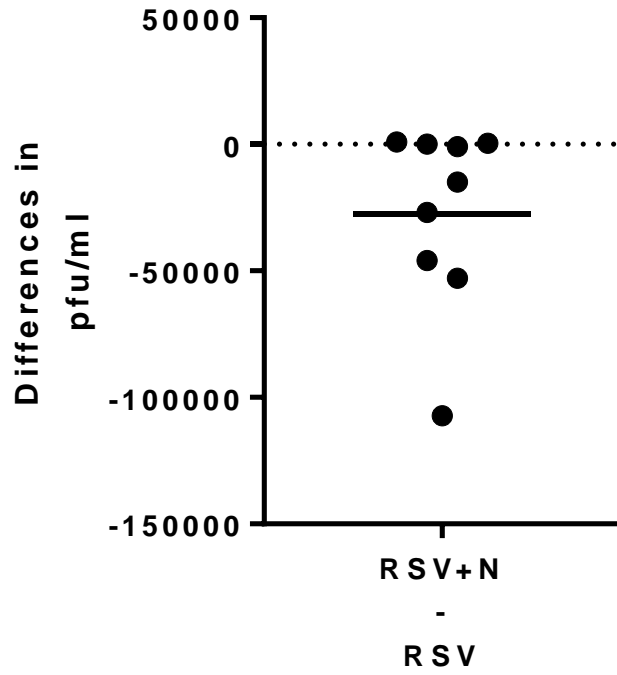


Figure S6 The difference in RSV viral titre between infected nAEC cultures after 4h with and without neutrophils as determined by (A) by plaque assay and (B) N gene copy number by qPCR. Data represents difference in counts from homologous RSV infected nAECs in absence of neutrophils.

A



B

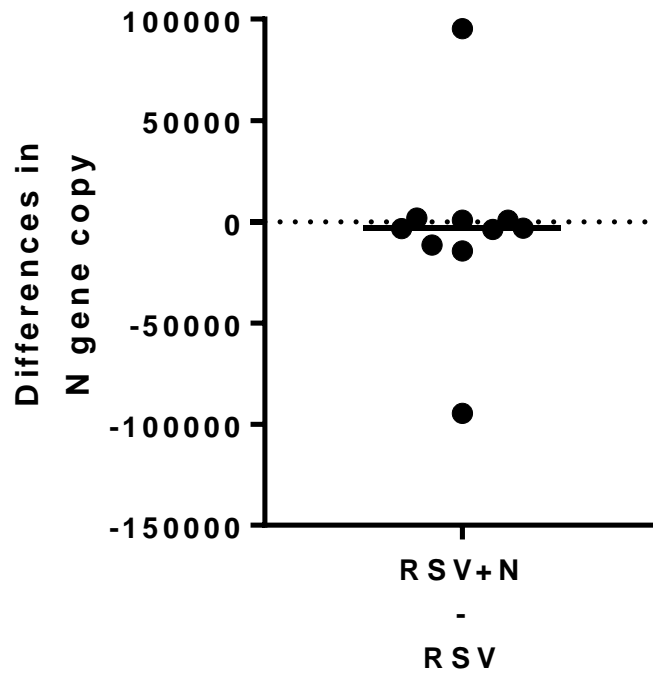
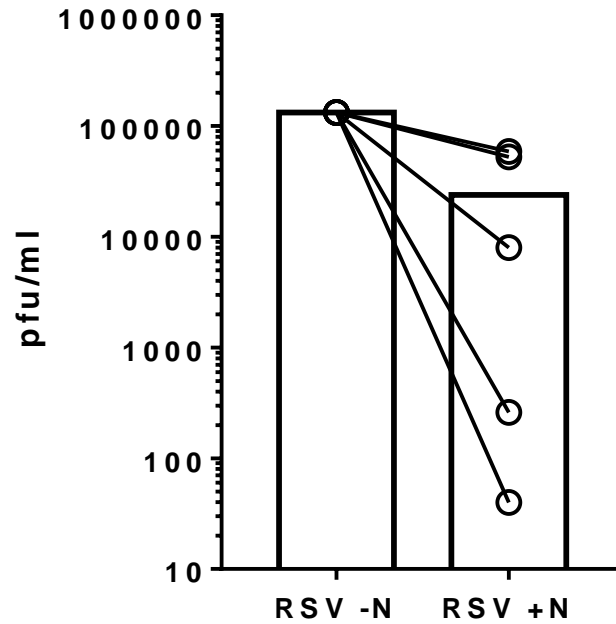


Figure S7 The effect of neutrophils alone (no AECs) on RSV viral titre determined by (A) by plaque assay and (B) N gene copy number by qPCR (n=5 neutrophil donors, 1-2 technical repeats, all data shown) after 4h in presence of neutrophils.

A



B

